2013

Development of a corn stover yield monitor

Byron Manternach
Iowa State University

Development of a corn stover yield monitor

by

Byron Nathan Manternach

A thesis submitted to the graduate faculty

in partial fulfillment of the requirements for the degree of

MASTER OF SCIENCE

Major: Agricultural Engineering

Program of Study Committee
Stuart J. Birrell, Major Professor
Matthew Darr
Steven Hoff

Iowa State University

Ames, Iowa

2013

TABLE OF CONTENTS

Page

LIST OF FIGURES

Page

LIST OF TABLES

Page

ACKNOWLEDGMENTS

I would like to thank Dr. Stuart Birrell for his direction and guidance throughout my research project. His insight and experience we invaluable in enabling me to complete my research. Also, I would like to thank Dr. Matt Darr and Dr. Steven Hoff for their support and guidance as well as serving on my program of study committee.

A thank you is also extended to my student colleague Daniel Murray for his assistance in conducting my research and testing. I greatly appreciate the long hours that he provided in helping me conduct my research.

My gratitude goes to my wife, Shelley Manternach, for her love and support during my research. I am grateful for her help in the field and her encouragement during my work.

CHAPTER 1.0 INTRODUCTION

Recent United States national energy policy has pushed for alternative energy sources from fossil fuels. Corn stover specifically has been targeted as a biomass feed stock that is currently readily available with 92.0 million acres planted (NASS 2011) in the United States and 75 million dry tons of corn stover available per year (Oak Ridge National Laboratory, 2005). Questions have begun to develop about the suitability of removing large amounts of corn stover from fields.

Concerns of sustainable stover harvest include the effects of corn stover removal on Soil Organic Carbon SOC and wind and water soil erosion. (Johnson et al., 2006; Wilhelm et al., 2007) To address these concerns; tools such as the revised universal soil loss equation 2 (RUSLE 2) can be used to predict safe removal rates (Andrews S., 2006; USDA-ARS. 2003). The RUSLE 2 determines a required amount of ground cover to be left on a field based on the amount of biomass above ground, soil type, soil slope, and field management practices.

The RUSLE 2 uses the yield and harvest index (HI) to calculate the amount of biomass above ground. The calculation of harvest index is shown in Equation 1:

$$\textbf{Equation 1: } Harvest\ Index = \frac{\text{Grain mass}}{Grain\ Mass + Stover\ Mass}$$

The typical harvest index for modern corn hybrids is 0.53 (Johnson et al., 2006). Weather and tillage practices can greatly affect the HI. In a thirteen year study by Linden et al., (1999) the HI of corn studied varied from 0.4 to 0.6 with a mean of 0.56. Weather effects such as hail (Haverson et al., 2002) and water stress (Prince et al., 2001) have also been shown to affect the HI of corn. An inaccurate HI value will result in inaccurate predictions for available corn stover and therefore cause inaccurate removal rates of corn stover. If the total amount of stover available is over predicted, this would result in unsustainable stover harvest and result in unacceptable soil erosion and SOC levels. If the amount of corn stover is under predicted the amount of stover removed may be less than the amount possible for

harvest. For this reason a more reliable system should be developed to measure the amount of stover in the field.

1.1 Literature Review

One of the earliest tools adopted for precision agriculture was the grain yield monitoring equipment in combines. The Ag Leader Yield Monitor 2000 was one of the first available on the go yield monitors and was introduced in 1992 (History Timeline 1992). This yield monitor used an impact plate at the top of the clean grain elevator to measure the impact force of the grain from the clean grain elevator (Yield Monitor 2000 Operators Manual). Other methods developed for measuring grain yield include the detection of grain volume on the slats of a clean grain elevator using the light attenuation of photo diodes (Pfeifer et al 1993; Chaplin et al. 2003).

In attempts to improve yield mapping quality Veal et al., (2004) examined the effectiveness of a feeder housing-based mass flow sensing system. This system measured the tension of the feeder house chain with the reasoning that increased chain tension would be associated with increased biomass flow. They concluded that chain tension could be used to produce more accurate spatial yield data and chain tension had a correlation coefficient R^2=.86 between biomass weight and sensor voltage.

Yield monitoring technology for grain harvest has been widely adopted in agriculture practices, but yield monitoring technology to measure biomass yields for the purposes of corn stover collection are not as readily available. The bulkiness of corn stover is similar to that of hay and forage, therefore, investigating the yield measuring methods used in hay and forage production may prove useful.

The development of yield monitoring technologies for hay and forage production machinery include balers, windrowers, and forage harvesters. Yield mapping technology for balers include measurements of bale velocity, weighing of the bale while on the bale chute and measurement of plunger force pulse width (Shinners et al 2000). Forage yield measurements were established by measuring conditioning roll force, conditioning roll

displacement, and crop impact force on the swath forming shield of a windrower (Shinners et al 2000 and 2003). Methods developed to measure yields using forage harvesters include the use of infa-red reflection and impact based measurements in the spout of a forage harvester. Currently the commercially available HarvestLab from John Deere utilizes infa-red reflection to measure forage yield and nutrients during harvest (Deere & Company, 2012).

Marrel et al. (2000) examined the effectiveness of a load cell connected to a hinged plate in the spout of a forage harvester. The hinged plate, the width of the spout was inserted in the bend of the spout and connected to a load cell. A "S" type load cell connected to the plate measured the impact force of the particles against the plate. Field experiments with this sensor were conducted by harvesting whole plant corn silage. High and low speed test runs were conducted to evaluate the sensor's effectiveness in measuring the sensor in measure the mass flow of material harvested by the forage harvester. A low pass filter was used to process the sensor response and then the processed signals were averaged to determine an experimental mass flow rate. A linear relationship between impact force and mass flow rate produced a R^2 of 0.948.

Later work by Savoie et al. (2002) utilized a capacitance-controlled oscillator to measure the moisture of the material in the spout of a forage harvester. In field experiments using wilted grass the impact sensor alone produced a R^2 of 0.951. Creating a prediction equation using both the response of the load cell and frequency drop of the capacitance-controlled oscillator increased the R^2 to 0.979 implying that predicting material moisture can improve the accuracy of an impact based mass flow sensor.

In spout methods work well for gathering all biomass available, but not well in a scenario where it is desired to return some or all biomass to the ground for a sustainable harvest of corn stover. The use of variable rate stover return technology would require the ability to measure the amount of corn stover in the combine before the stover enters a wagon or collection mechanism.

Expanding the method of using a force plate to calculate mass flow in a forage harvester spout and windrower, a similar method could be developed for use in a combine.

An instrumented impact plate could be installed in the combine at a location where the stover flowing through the combine would contact the plate causing a measurable force on the plate.

CHAPTER 2.0 OBJECTIVES

The objective of this research was to determine if corn stover mass flow through a combine could be measured by the impact force of the stover leaving the combine rotor discharge beater. To achieve this project goal, four separate objectives were determined:

- Determine the best way to instrument and orient an impact plate in the threshing area of the combine.
- Determine if impact force of corn stover on the impact plate sensor can be used to measure the mass flow rate of the corn stover.
- Investigate the interactions between sensor response, stover flow rate, plant cut height, and stover moisture content.
- Develop a mass flow rate prediction equation based on sensor response.

CHAPTER 3.0 SENSOR DESIGN AND DEVELOPMENT

Development of the impact plate sensor began by designing a curved steel plate that would fit behind the rotor discharge beater of a John Deere 9860 STS combine. The stover leaving the combine rotor is propelled by the rotor discharge beater away from the rotor and then guided to the throat of the chopper for size reduction and expulsion from the combine. Ideally the impact plate would be designed and installed to collect the normal forces from the impacting stover. This design however, was not possible because a plate designed to collect the normal forces of the impacting corn stover would not allow stover leaving bouncing off the impact plate to be guided to the chopper of the combine. A modified impact plate design would provide minimal interference with the material flow path and allow for impact forces of the stover to still be measured. An impact plate was designed that would fit behind the rotor discharge beater and cover the width of the discharge beater. Figure 1 shows a solid model of the location of the impact force sensor and the stover flow path.

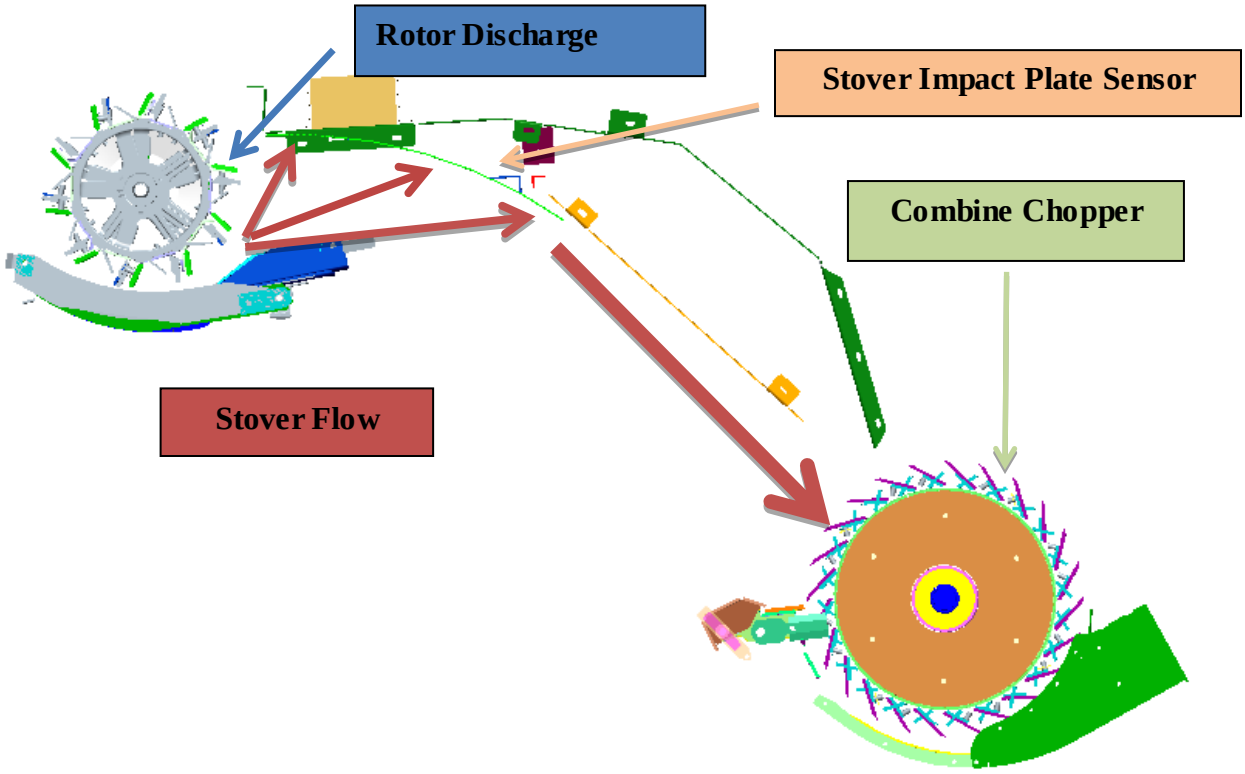

Figure 1: A solid model of the impact plate sensor as installed in the combine.

Instrumentation of the impact plate required that the impact force of corn stover hitting the impact plate at any location about the radius of the plate to be measured. Two instrumentation methods were considered and then analyzed to determine which method would have greater ability to accurately measure stover impact force, across the operating range of the system. The two examined methods were as follows:

1. Hinge the top edge of the impact plate and instrumenting the plate with a load cell in each bottom corner. The load cell orientation could be vertical or horizontal.
2. Instrument each of the bottom corners of the impact plate with two load cells. One load cell to measure the horizontal impact force and another to measure the vertical impact force. Then instrumenting each of the top corners of the impact plate with load cells oriented at 45 degree angles. The forces of these angled load cells could be resolved into horizontal and vertical force components and combined with the lower load cells.

Solid model drawings were utilized to determine the geometry of the impact plate installed in the combine. For analysis seven potential trajectories of particles were considered. The first impact point was located at the leading edge of the impact plate and the seventh point was located at the bottom of the impact plate. The remaining five points were spaced evenly along the radius of the plate. The stover flow paths from the rotor discharge beater to the impact plate were determined by drawing vectors tangent to the rotor discharge beater and impacting the impact plate at the identified impact locations. Then the necessary dimensions were calculated using model drawings. Figure 2 shows the impact plate in the intended installation location, the analyzed impact points on the impact plate, and the impact vectors of the stover from the discharge beater to the impact plate. Figure 2 also shows the horizontal and vertical measurements for impact location 2.

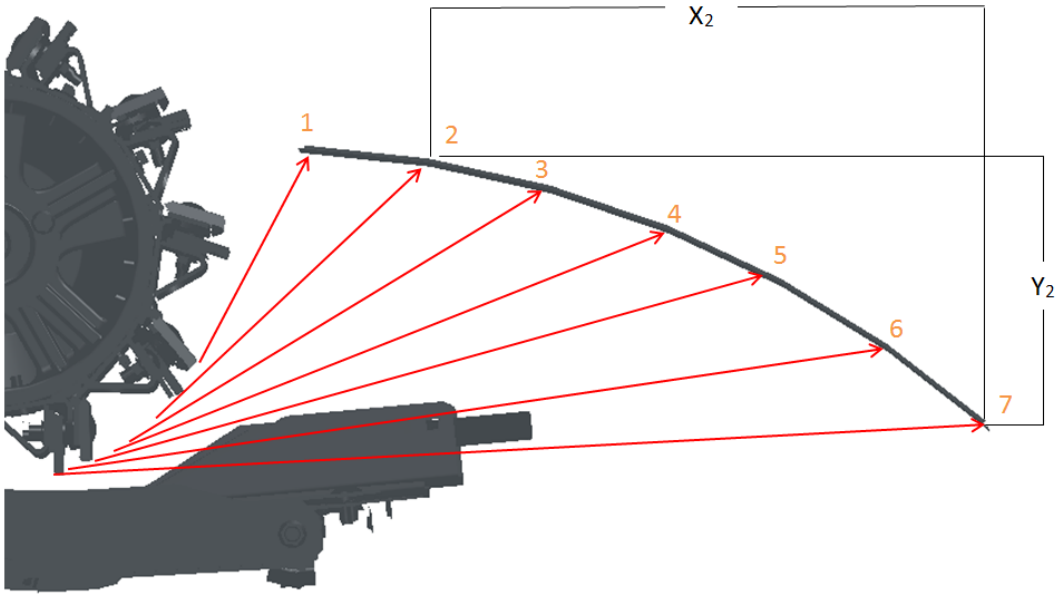

Figure 2: Diagram of impact plate showing impact vectors, analyzed impact locations, and referenced dimensions of impact locations. (Measurements only shown for location 2 for clarity)

To evaluate the impact forces at the impact points, impact angles and references to the horizontal and vertical axis needed were to be determined. Figure 3 shows example measurements from impact location 2. The red arrow indicates the impact vector at location 2 of the stover on the impact plate. The X and Y axis are shown in orange and the blue line is the line tangent to the curvature of the impact plate at location 2. The angle between the impact vector and the X axis was identified as θ. The angle between the impact vector and the tangent line of the curvature at the analyzed impact point was identified as α. The impact force vector was shown in green and was perpendicular to the tangent line of the curvature at the analyzed impact point. The angle of incidence was identified as the angle γ.

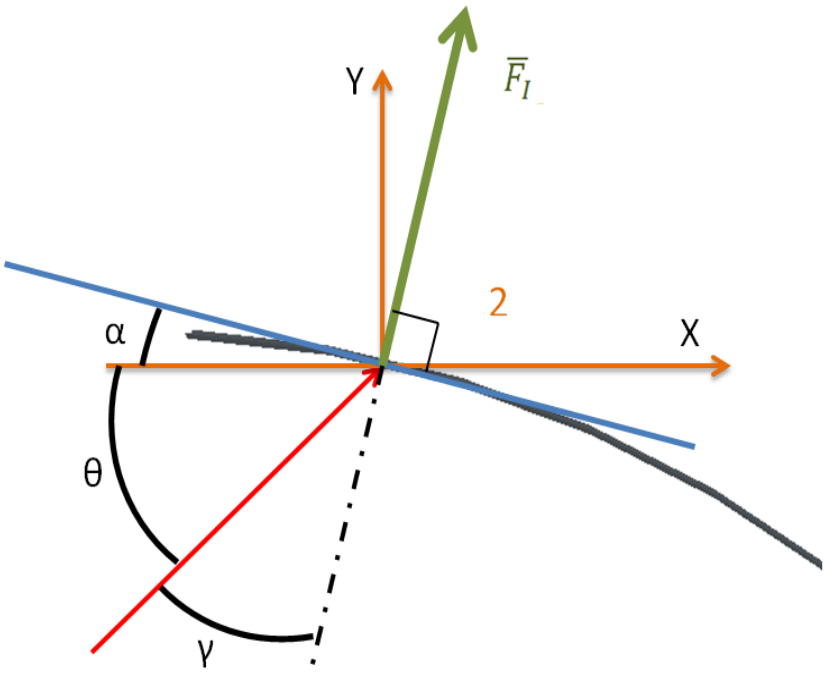

Figure 3: Diagram of angle measurements for stover impact location 2.

To calculate the impact force of the stover on the impact plate at the seven locations the following analysis was conducted. For the analysis of instrumentation method 1 impact point number 1 was considered the hinge point and impact point 7 was considered the instrumentation point for a load cell to measure the impact force of the stover. Instrumentation method 2 used impact location 1 as an instrumentation point for the load cell oriented at 45 degrees and impact location 7 as an instrumentation point for the horizontally and vertically oriented load cells. The impulse momentum equation was used to calculate the impact force. The impulse momentum equation is shown in Equation 2.

Equation 2: $\Delta \boldsymbol{P_I} = \boldsymbol{mv_1 \sin(90 - \gamma) - mv_2 \sin(90 - \gamma)}$

Where:

$\Delta \boldsymbol{P}_I$ = the impact momentum

m= the mass of the impacting stover particle

v_1= the magnitude of the velocity vector of the particle just before impact

γ= the angle of incidence of the stover particle, this angle was measured normal to the tangent of the curvatures radius at the point of impact

v_2= the magnitude of the velocity vector of the stover particle just after impact

The impact force of a stover particle can be calculated using Equation 3.

Equation 3: $\overline{F_I} = \frac{mv_1 \sin(90-\gamma) - mv_2 \sin(90-\gamma)}{\Delta t}$

Where:

$\overline{F_I}$= the average impact force of the stover particle

Δt= the time of the particle impact

Using a coefficient of restitution shown in Equation 4, Equation 3 becomes Equation 5.

Equation 4: $CR = \frac{v_2}{v_1}$

Where:

CR= the coefficient of restitution

Equation 5: $\overline{F_I} = \frac{mv_1 \sin(90-\gamma) - mCRv_1 \sin(90-\gamma)}{\Delta t}$

For every point analyzed along the impact plate the mass of the particle, the magnitude of the velocity of the particle before impact, and coefficient of restitution were assumed to be constant. Using those assumptions Equation 5 can then be simplified to Equation 6.

Equation 6: $\overline{F_I} * C = \sin(90 - \gamma)$

Where:

C= a constant seen in Equation 7.

Equation 7: $C = \frac{\Delta t}{(1-CR)*m*v_1}$

Table 1 shows the angles determined from model drawings and the relative impact forces calculated with Equation 6. The angle α is the angle in degrees from the horizontal to the tangent line of the impact plate radius at the impact points. The angle θ is the angle in degrees from the stover impact vector and the horizontal axis. The angle γ is the angle of incidence for the impact point. The calculated mean impact forces shown in Table 1 show how the angle of incidence of the stover particles affects the transferred mean impact force to the impact plate. A smaller angle of incidence results in greater force transferred to the impact plate confirming that a normal impact of stover would result in the most force transferred to the impact plate. Note that only impact forces were evaluated and no sliding forces were analyzed.

Table 1: Relative impact force at the analyzed impact locations, based on angle of tangent line (α), angle of impact vector (θ), both with respect to horizontal axis and angle of incidence (γ).

Impact Location	α	θ	γ	Relative Impact Force
1	0	66	24	0.91355
2	6	46	38	0.78801
3	14	33	43	0.73135
4	21	24	45	0.70711
5	28	17	45	0.70711
6	33	11	46	0.69466
7	38	6	46	0.69466

Using the relative impact forces from above; the instrumentation methods could be evaluated to determine what method would be best to instrument the impact plate. Detailed equations to develop the measured force responses are shown in the Appendix A. Figure 4 shows the force response of the stover at the impact points and the measured force response at the impact points using Instrumentation Method 1. Component force response values are the component forces acting on the impact plate caused by the impacting stover. Component measured force response values are the force values measured by the load cells. Vertical

force responses were determined by using vertically oriented load cells at point 7 and horizontal force responses were determined by using horizontally oriented load cells at point 7. The vertical force response varied 0.37 in measured relative impact force from impact point 1 to impact point 7. The vertical measured relative mean impact force response had the opposite trend of the stover vertical force response. The vertical measured force response varied 0.44 from impact point 1 to impact point 7. The stover horizontal force response varied 0.42 in horizontal force response from point 1 to point 7. The measured horizontal force response varied 0.70 from impact location 1 to impact location 7 and had a similar trend to the stover horizontal force response. Both the vertical and horizontal measured force responses trend closer to the stover force responses as the impact point approached the sensor location. If instrumentation Method 1 was selected the vertical load cell orientation would be best because the measured vertical force response had less variation between impact points 1 and 7. The horizontal measured force response had a greater variation from impact points 1 to 7 and crossed the origin of the vertical axis causing measured impact forces from impact point 1 to 2 subtract from the measured impact forces from impact point 3 to 7.

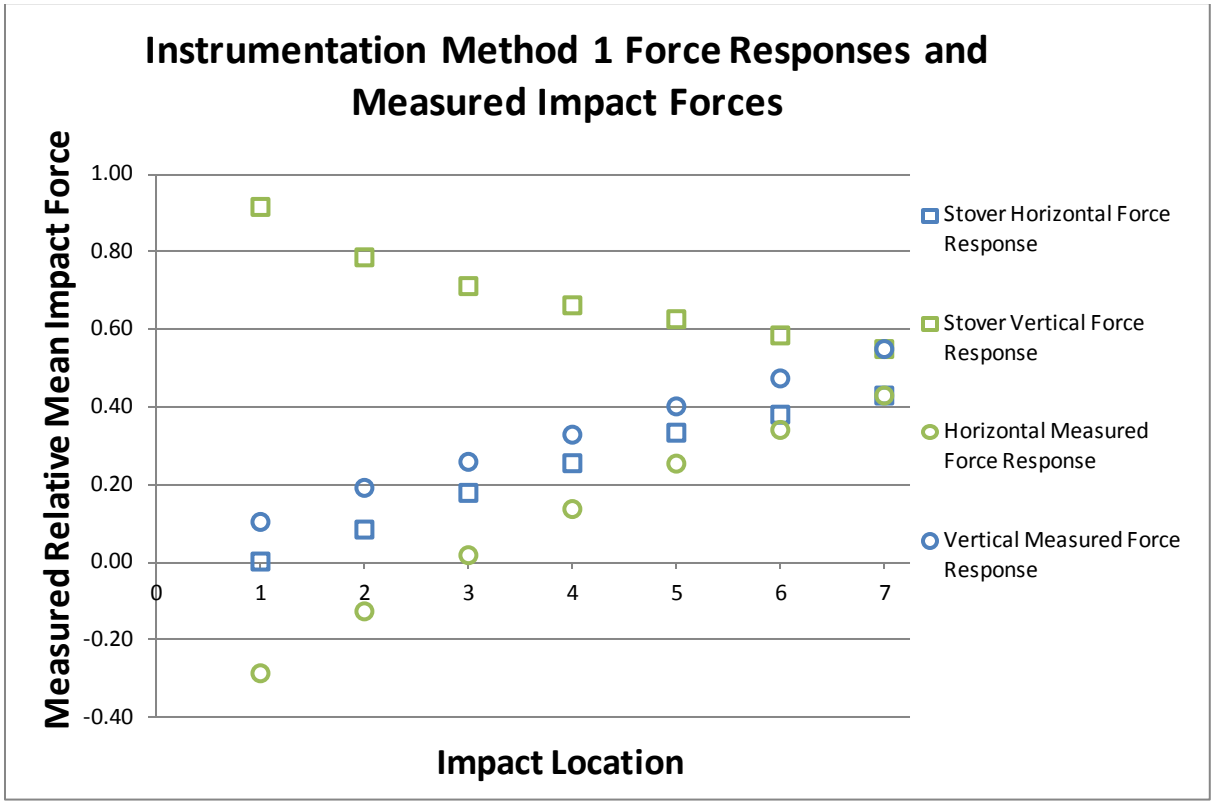

Figure 4: Instrumentation Method 1 measured impact forces response and stover force responses for impact locations.

Analysis of Instrumentation Method 2 showed that the horizontal, vertical, and magnitude measured force responses aligned with the horizontal, vertical, and magnitude force responses. Figure 5 shows the force response of the stover and the measured force response for Instrumentation Method 2. The relative impact force from Table 1 was the same as the force response magnitude. The magnitude force response varied 0.20 in force response from impact point 1 to impact point 7. The variation in the magnitude response from point 3 to 7 was 0.04 on the measured relative mean impact force scale. This implies that there would be little change in the magnitude sensor response between impact points 3 to 7 which would minimize the variation in the magnitude sensor response due to impact location. For this reason Instrumentation Method 2 was chosen as the instrumentation method for the impact plate.

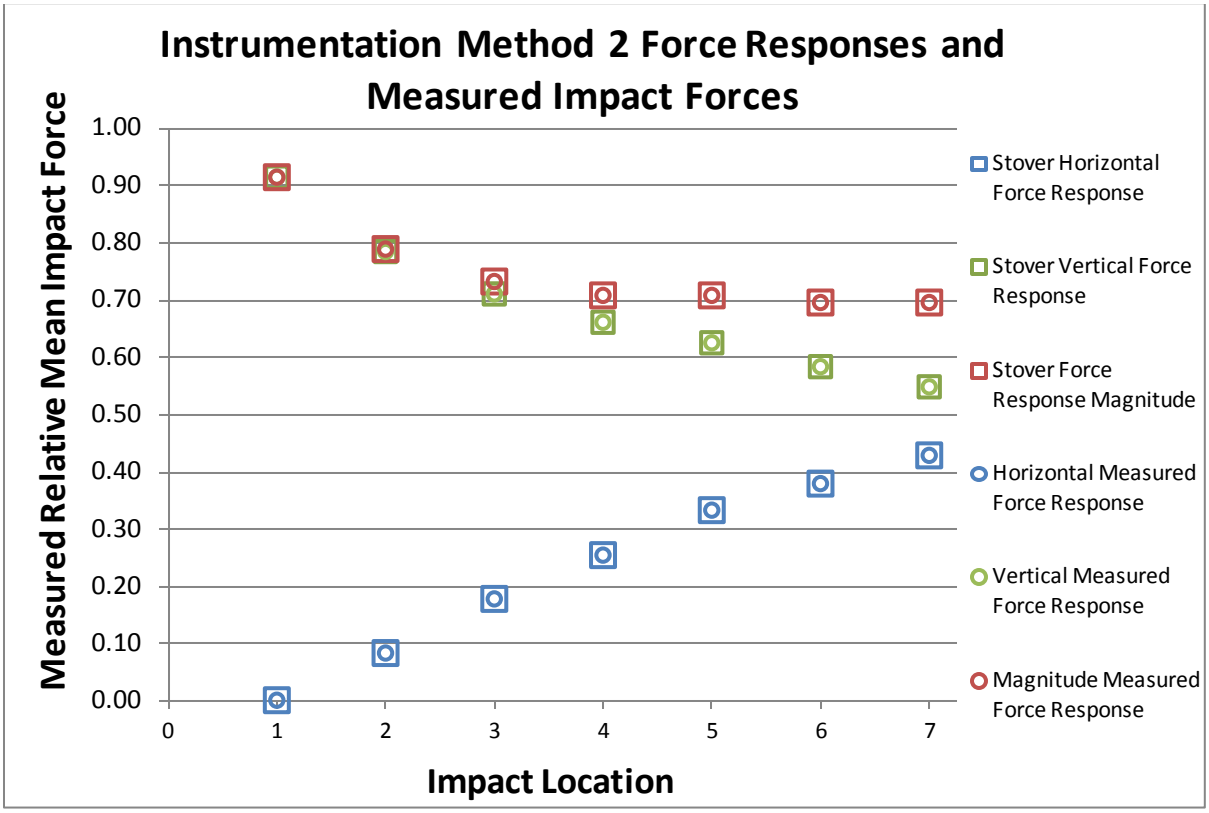

Figure 5: Instrumentation Method 2 measured impact forces response and stover force responses for impact locations.

Six MLP-300 (Transducer Techniques, Temecula, CA) load cells were utilized to measure the forces on the impact plate created by the contacting material. The MLP-300 is a tension compression load cell with a maximum load of 300 lbs. Attaching the lower corners of the impact plate to the combine was done by bolting a MLP-300 load cell to an angle bracket welded to the impact plate. This load cell was oriented to collect horizontal force components on the impact plate. A right angle bracket connected the horizontal load cell to a load cell oriented vertically. This vertically oriented load cell was to measure the vertical force components on the plate. The vertically oriented load cell was then connected to the frame structure of the combine. Figure 6 shows the method of the lower corner impact plate's attachment combine frame structure.

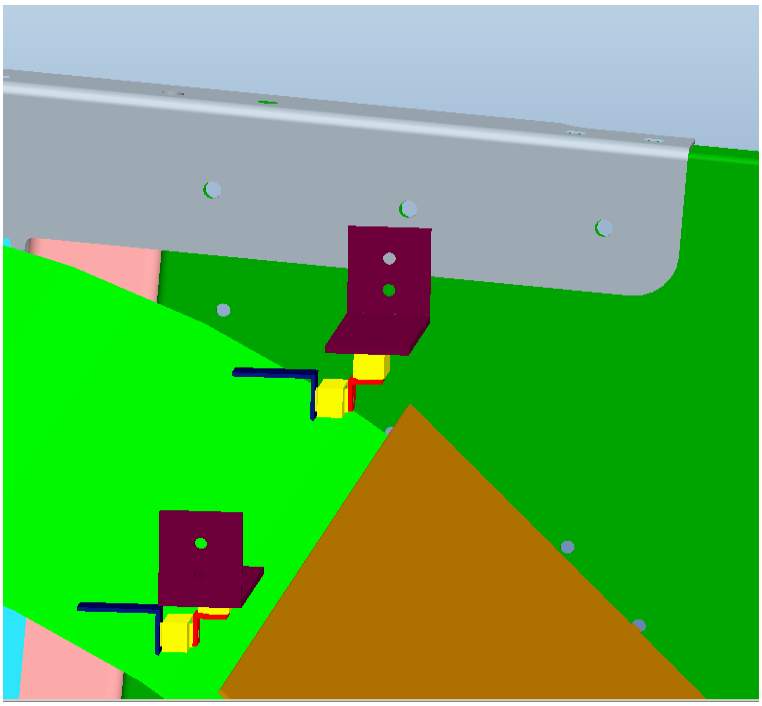

Figure 6: Pro/E model showing the load cell orientation and connection of the bottom corners of the impact plate.

A MLP-300 load cell was utilized in each top corner of the impact plate to connect the impact plate to the frame structure of the combine. These load cells were oriented at 45 degree angles. Linkages were developed utilizing ball joint rod ends and turnbuckles to connect the impact plate to the combine frame structure. Incorporated into each linkage was a MLP-300 load cell. The ball joint ends allowed for only the forces in line with the linkages to be measured and other forces to be transferred to the lower load cells. The turnbuckles allowed for the lengths of the linkages to be adjusted so that the gap between the top leading edge of the impact plate and the threshing area ceiling could be minimized without cause contact between the impact plate and threshing areas ceiling.

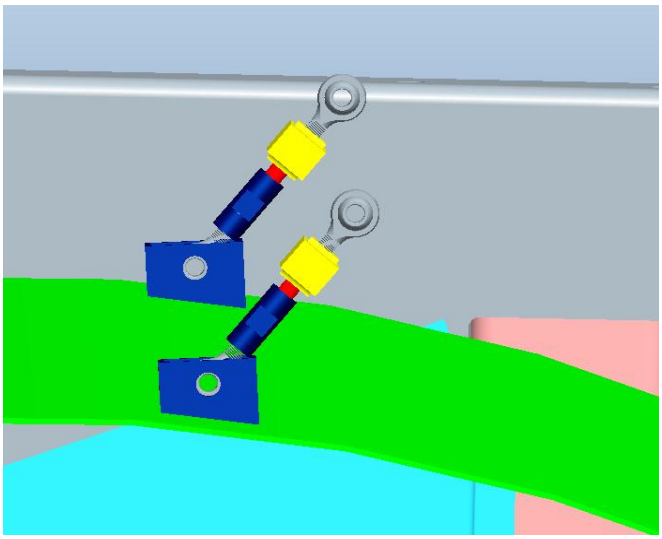

Figure 7: Pro/E model showing load cell orientation and connection method at top corners of the impact plate.

CHAPTER 4.0 EQUIPMENT AND MATERIALS

4.1 Single Pass Dual Stream Combine Harvester

The John Deere 9860 STS combine utilized for the impact plate sensor development was equipped with a single pass dual stream attachment previously co-developed by Iowa State University and Deere & Company (Moline, IL). The attachment permitted the collection of corn stover while conducting the traditional grain harvest. Major components of the combine that remained unmodified including the feeder house, rotor, and concaves. The dual stream stover collection system consisted of a dual axis chopper, blower, and spout. The blower and spout were similar to that found on a forage harvester. The purpose of the dual axis chopper was to produce a smaller particle size than a standard combine chopper making the stover better able to be processed at a later energy conversion. The blower and spout attached behind the chopper allowed the stover to be transferred to a wagon or truck for collection.

4.2 Corn Head

The corn head used in the fall of 2010 and 2011 was a modified John Deere 612C chopping corn head. This head was a 12 row corn head with 30" row spacing. The standard gathering chains were replaced with gathering belts connected to circular blades at the front of the row unit in order to cut the corn plant at the entry point of the head and pull the cut portion of the plant into the head.

4.3 Data Acquisition System

In order to collect data to evaluate the effectiveness of the impact plate sensor, responses from the load cells and other machine functions needed to be recorded. During the fall of 2010, an eDAQ (Somat., Marlboro, MA) and an Athena II PC-104 computer from (Diamond Systems., Mountain View, CA) were utilized for data acquisition. Six bridge channels of the eDAQ were used to record the response of the load cells. The load cells were connected to the bridge channels of the eDAQ and calibrated using calibrations provided

with the load cells. The load cells were connected to the bridge ports so that a compressive force on the load cell caused a positive force reading. The load cell response was recorded in pounds force. A Garmin GPS18 PC (Garmin Ltd., Olathe, KS) was connected to the GPS channel of the eDAQ to record position of the combine and UTC time. The sampling rate of the eDAQ was set to 1000 HZ.

The PC-104 computer included the following components: Athena II single board computer/data acquisition system, USB-4300 Measurement Computing counter module (Measurement Computing, Norton, MA), and CANUSB convertor (Lawicel AB, Tyringe, Sweden). The Athena II was equipped with a 16 bit analog to digital converter for analog signals. The USB-4300 counter was used for all counting operations. The CANUSB convertor was used for accessing yield data from the vehicle CAN Bus. GPS information was accessed from the Green Star SF1 GPS unit. A Visual Basic interface was developed and used to operate the PC-104 data acquisition components. The Athena ll was set for a recording frequency of 10 Hz. This recording frequency was the maximum recording speed due to the computing load on the Athena II computer.

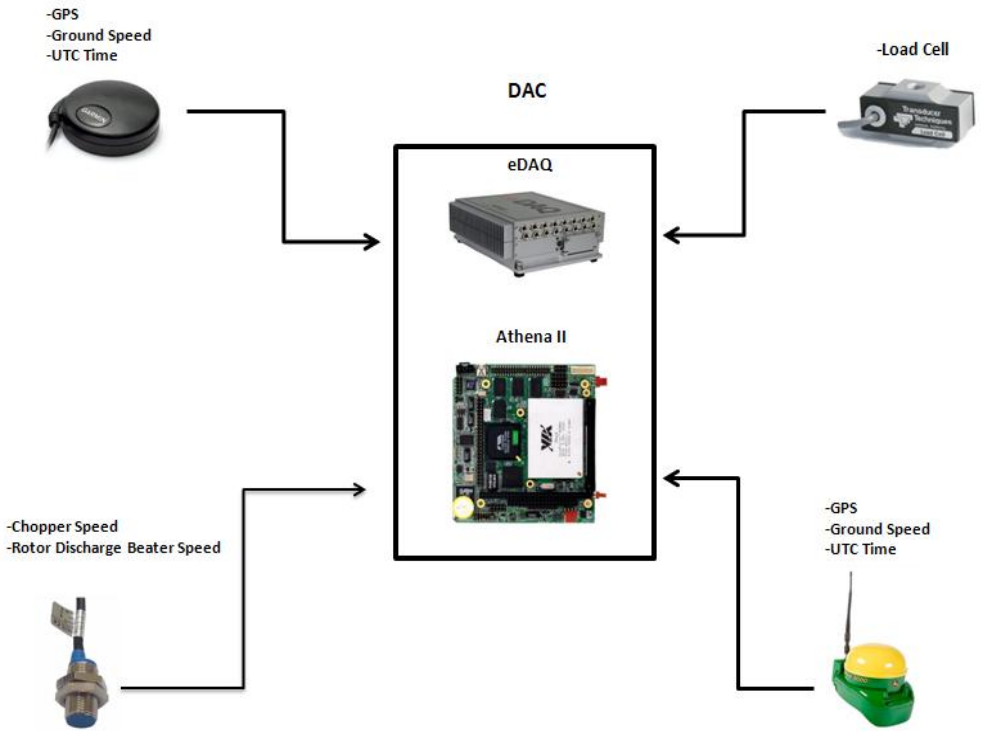

Figure 8: Diagram of Fall 2010 data acquisition system.

During the summer and fall of 2011, a PC 104, Model 518 Smart Analog Digital card (Sensoray, Tigard, OR) was utilized. This data acquisition card was linked to the Athena II computer board through the PC 104 bus. The six load cells were connected to the load channels on the Smart Analog Digital Card and calibrated using the procedures defined in the user's guide (Sensoray, 2001). The load cells were connected to the load cell channels so that a compressive force on the load cells would cause a negative force reading. The Smart board was set up to filter incoming data at ten Hz because this was the maximum recording speed of the Athena II computer. The response of the load cells was recorded in pounds force.

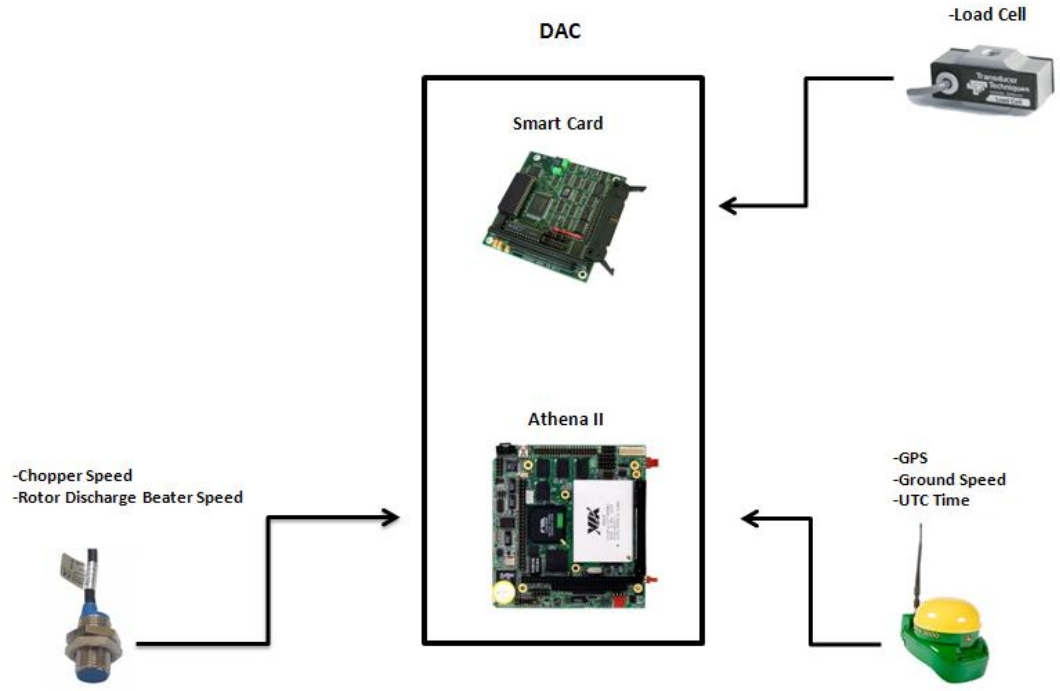

Figure 9: Diagram of Summer 2011 and Fall 2011 data acquisition system.

All grain weights were weighed in a load cell instrumented grain cart (Digi-Star., Fort Atkinson, WI) with a resolution of ±5 lbs. All harvested stover was collected in a forage wagon (Meyer., Dorchester WI) equipped with an EZ 2400 scale head and instrumented with four CT30KTC weigh bars (Digi-Star., Fort Atkinson, WI). The resolution of the EZ 2400 scale was ±10 lbs.

CHAPTER 5.0 METHODS AND PROCEDURES

Testing of the impact plate stover yield sensor was conducted in three iterations: field testing in the fall of 2010, semi stationary testing in the summer of 2011, and field testing in the fall of 2011. Initial testing in the fall of 2010 was conducted to collect impact plate data for evaluation and development recommendations. Testing in the summer of 2011 was conducted to evaluate the effects of stover moisture on the impact plate load cell response. Testing in the fall of 2011 was conducted to verify pervious results and further evaluate and develop the impact plate based mass flow sensor.

5.1 Testing Procedures

5.1.1 Fall 2010 Field Testing Procedure

Initial field testing took place in November of 2010 on the Iowa State University Agricultural Engineering research farm west of Ames, Iowa. The corn variety was DeKalb DKC 61-22 planted in the north south direction. Fall 2010 test procedures were conducted as follows: First the scale of the stover collection wagon was tared. The combine separator and head were engaged and the engine speed increased to operating speed. Recording of the eDAQ and Athena II data acquisition systems were started. Then the combine moved forward to harvest the corn at the targeted operating ground speed for the test run. During the test run the corn stover leaving the combine was blown into the collection wagon being pulled beside the combine. The forward motion of the combine was stopped once reaching the end of the plot and full engine speed was maintained until the combine was cleaned out. The data acquisition systems were then stopped and the threshing system and header were disengaged. The weight of the collected stover was recorded and two samples of the stover were taken for moisture analysis. The moistures of the samples were measured and an average run moisture was calculated. The grain was weighed and recorded.

5.1.2 Summer 2011 Stationary Testing Procedures

Dry conditions and a late harvest did not allow for a wide variety of moistures to be tested in the fall of 2010; therefore, testing was conducted in the summer of 2011 to evaluate the effects of moisture on the stover yield sensor. Testing in the summer did not allow for the harvesting of standing corn so an alternative harvest method needed to be developed. A stationary test plan was developed that utilized large square (3'X4'X7') corn stover bales that were baled in the Ames, Iowa region. Bales were made in the fall of 2010 and were baled at approximately ten percent moisture content and stored under tarps. The bales used in the testing were harvested with similar shredding and baling procedures, but enough bales from the same field were not available to conduct the entire test. Moisture of the stover was then artificially increased using the following procedures. The lower moisture level was set as the initial bale moisture and was assumed to be ten percent moisture. Maximum nominal moisture of twenty percent was limited because of feeding problems of the stover on the pickup head occurred above this moisture level. The mid moisture level of fifteen percent nominal moisture was determined by selecting the middle of the low and high moisture levels. Actual stover moistures were determined by taking samples during testing for analysis.

During the Summer of 2011 testing the test setup did not allow for ground speed to be used to determine the flow rate of stover through the combine, therefore flow rate of the stover was determined by the capacity of the combine. For the high flow rate test runs the combine was kept at full capacity. Full capacity was determined as operating the combine so that the engine speed was 100 rpm below high engine speed. For the low flow rate test runs the combine was operated at low capacity. Low capacity operations were determined as holding the flow rate of material through the combine so that the engine rpms did not drop below high engine speed. For mid flow rate test runs the capacity of the combine was held between the high and low capacity levels. During testing the capacity of the combine was greater for the dry material than the wet material.

Testing began by preparing the corn stover for the test run. Two large square corn stalk bales were loaded into the TMR vertical mixer. Using the TMR scale the weight of the

bales was recorded. If the moisture level of the bale was to be increased, the amount of water to be added to the bales was determined by assuming the current stover moisture was ten percent and then calculating the amount of water necessary to achieve the desired nominal moisture. The bales were then processed in the mixer for three minutes and water was added at this time, if necessary to increase the stover moisture. The purpose of processing the bales was to break the flakes of bale apart and not to reduce the size of the corn stover. Once the bales were processed they were laid out in a windrow with the TMR conveyor.

To run the test the combine was attached to a John Deere (Deere and Co., Moline, IL) Model 613 P belt pickup head and the head was used to pick up the windrow created by the TMR. The weight of the collection wagon was zeroed and the DAQ was started. The separator and header of the combine was started and increased to operating speed. Next, a toggle indicating the baseline interval was triggered on the DAC interface. This toggle identified when the combine was running at a steady state and no material was passing through the machine. The base line interval indicator was allowed to run for six seconds and then ended. Next, the run interval toggle was triggered and the combine was driven forward into the windrow. The run interval toggle indicated when stover was passing through the combine. The combine was operated at a forward speed depending on the targeted flow rate. During the test run the stover was blown in to the Meyer forage box. At the end of the windrow the forward motion of the combine was stopped and the run interval toggled cleared. Once the combine had cleaned out the DAQ was stopped and the combine header and separator were disengaged. The weight of the Meyer forage box was recorded and a sample of the stover was taken to determine the actual moisture of the tested stover.

5.1.3 Fall 2011 Field Testing Procedure

Field testing in the fall of 2011 took place on the Iowa State University Agricultural Engineering research farm west of Ames, Iowa. The corn variety was Pioneer PO528 XR planted in the north south direction. Field testing was conducted in the fall of 2011 to verify previous results and further examine the effectiveness of the stover yield sensor in predicting the stover flow rate though the combine.

The procedure used for each test plot in the Fall 2011 testing is described in the following paragraph. At the beginning of each test plot, the head height of the combine was adjusted according to the height specified for the test run. The scale of the stover wagon was tared. The DAC was started and the separator and header of the combine were engaged. The combine engine was brought to operating speed and the base line toggle indicator was triggered. After six seconds the base line toggle was stopped and the run interval indicator was engaged. The combine then moved forward to harvest the crop and maintained the proper ground speed specified for the test run. Once the combine reached the end of the test plot the forward motion of the combine was stopped and the run interval was stopped. Once the combine had cleaned out the engine speed of the combine was slowed and the thresher and header were disengaged and the DAC was stopped. Stover and grain weights were recorded and a stover sample was taken from the stover collected in the wagon for moisture analysis.

5.2 Data Processing Techniques

Data from impact plate testing for all three tests iterations were processed in the following fashion. Moisture calculations for the collected stover samples were calculated on a wet basis. The stover weights from the stover collection wagon were divided by the run time of each test to calculate an average flow rate of stover through the combine. Data files from the Fall 2010 testing were prepared for analysis using the following techniques. EDAQ files from the fall of 2010 were converted to Microsoft Excel files for processing. Once converted the base line and run interval of the eDAQ and Athena II files were identified. The purpose of the using the base line was to account for the offset in each load cell's value. The baseline interval was identified as the portion of the data file where the combine threshing system and header were running at operating speed without any crop entering or passing through the combine. The run interval for each test run was identified as the portion of the data file where the combine was harvesting crop. These intervals were identified by using the ground speed of the combine recorded by the GPS and the engine speed of the combine. The base line and run intervals of the data files from the summer and fall of 2011 were identified using the toggles used during testing. Data collected by the Athena II data

acquisition system including ground speed, chopper speed, and beater speed were averaged over the run interval and this average value was recorded as the value for each test run.

Data from the load cells from each test run was processed using the following techniques. The identified baseline interval was averaged for each load cell. The baseline average from each load cell was then subtracted from the corresponding load cell's value at each time stamp during the run interval to account for the zero offset of the load cells. Adjusted load cell values at each time stamp were then broken down into vertical and horizontal force components. Also the overall force magnitude of each load cell was calculated for every time stamp. These horizontal, vertical, and magnitude forces were then averaged over the identified run interval. The average values were then used as the values for the test run.

5.2.1 Statistical Analysis

Statistical models were created in the statistical software program JMP. Initial models were created using stepwise model development with full factorials of all variables. Variables were then removed from the produced models until explanatory terms in the prediction models met the 0.05 level of significance. Variable components used in interaction variables that did not meet the 0.05 level of significance were removed and the interaction models including the non-significant variable were also removed. The adjusted R^2 values are presented for each model to adjust for the different number of explanatory term in each model. Using the adjusted R^2 allows for models of different sizes to be compared.

The variables used in the prediction models were stover moisture, chopper speed, and values calculated from the load cells of the impact plate. The speed sensor used to record the speed of the discharge beater did not operate correctly during the Summer 2011 and Fall 2011 testing. The rotor discharge beater and combine chopper were driven from the same power shaft using belts so their speeds were proportional. The chopper speed sensor was much more robust and for this reason the speed of the chopper was used in the statistical analysis. Uncertainty of data values were developed using Taylor Series Expansion.

Detailed equations of the Taylor Series Expansion for stover moisture, chopper speed, and load cell values are shown in Appendix B.

5.3 Design of Experiments

5.3.1 Fall 2010 Design of Experiment

The key parameter identified for testing during Fall 2010 testing was stover flow rate through the combine. The flow rate of stover through the combine was controlled by adjusting the forward ground speed of the combine. All other parameters such as header height and combine threshing speed were held constant. The testing of the mass flow sensor was conducted in conjunction with testing of the dual axis chopper. Four configurations of the chopper were tested. Two ground speeds (2 mph and 4 mph) were tested with each chopper configuration and three randomized repetitions were conducted at each ground speed.

Table 2: Randomized block diagram for Fall 2010 field testing.

Treatment	Ground Speed (Mph)
1	2
2	4

5.3.2 Summer 2011 Design of Experiments

For testing in the summer of 2011 stover moisture and stover flow rate through the combine were identified as key parameters to evaluate. The moisture levels were blocked and the block order was randomized. The flow rates within each moisture level were randomized. Three repetitions of the nine treatments were conducted.

Table 3: Randomized block Design of Experiments for Summer 2011 testing.

Treatment	Moisture Level	Flow rate
1	Low	Low
2		Mid

3		High
4	Mid	Low
5		Mid
6		High
7	High	Low
8		Mid
9		High

5.3.3 Fall 2011 Design of Experiments

Testing conducted in the fall of 2011 incorporated three key testing parameters composed of stover moisture level, stover flow rate, and plant cut height. In the design of experiments the three moisture levels would be blocked and the moisture levels would be altered by varying the harvest date of the corn. Moisture level would be varied by having an early season harvest, mid-season harvest, and late season harvest of the corn. The cut height of the corn crop was set to a low or high cut height to examine the effects of cut height on the MOG mass flow sensors. The low cut setting was achieved by setting the corn head within a few inches from the ground. During the low cut, height stalk of the corn was cut approximately 14 inches from the ground. The high cut was conducted by setting the cutting disks of the head just below the ears of the corn plant. During the high cut, height the corn plant was cut approximately 25 inches from the ground. The flow rate of stover through the machine was varied by adjusting the ground speed of the combine. Target ground speeds of 2 mph and 4 mph were set.

Three replications were tested for each specific treatment. Because the moisture levels of the corn could not be randomized, the design of experiments was set up as a randomized block design with the corn moisture being blocked. The ground speed and head height were randomized for a total of twelve treatments.

Table 4: Randomized block Design of Experiments for Fall 2011 field testing.

Treatment	Moisture Level	Ground Speed (Mph)	Head Height
1	High	2	Low

2			High
3		4	Low
4			High
5	Mid	2	Low
6			High
7		4	Low
8			High
9	Low	2	Low
10			High
11		4	Low
12			High

CHAPTER 6.0 RESULTS AND DISCUSION

6.1 Mass Flow Sensor Response

Examination of the data collected showed a definite response of the load cells connected to the impact plate when stover was contacting the impact plate. Figure 10 shows a test run conducted in the fall of 2011. The response of the sensors shows a large amount of noise in the load cell signal, but there is a definite trend in the load cell response during the run interval of the test run. Since the material flow resulted in greater compressive force on the load cell, the load cell reading would decrease as material flow increased.

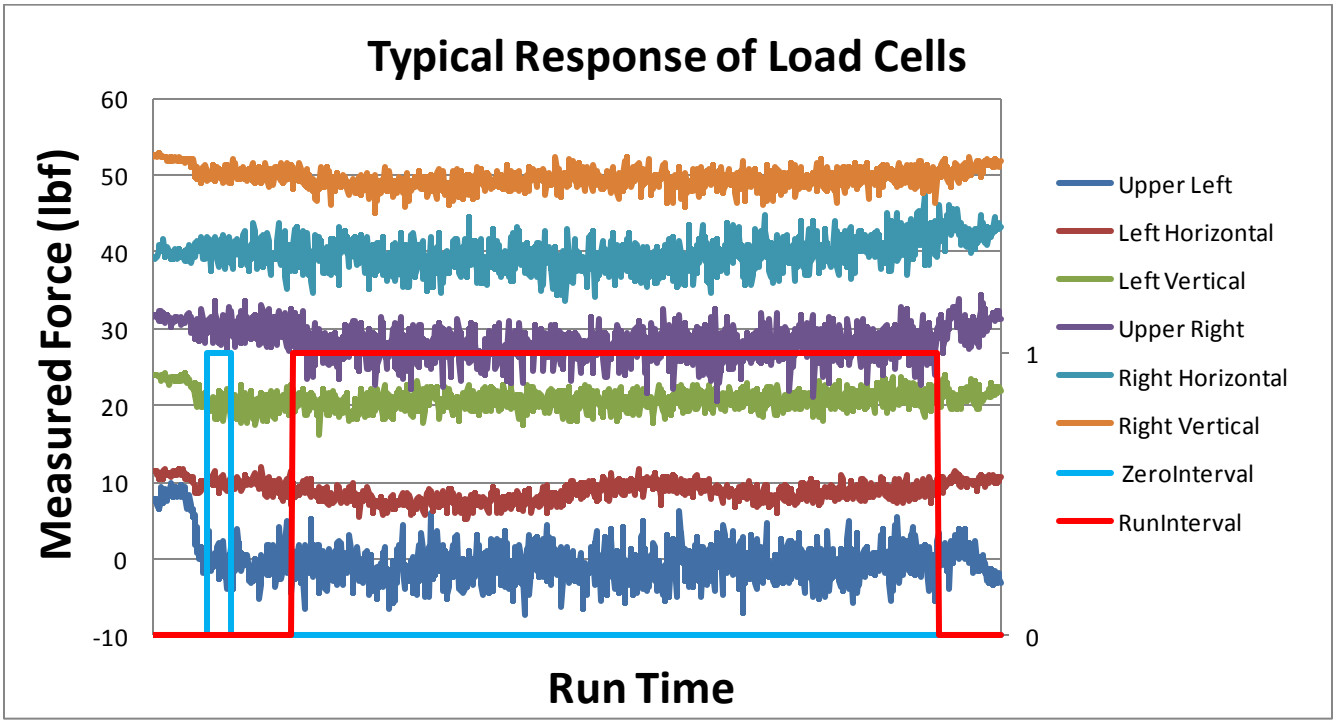

Figure 10: Typical response of individual load cells during a test run.

(Individual load cell traces have been shifted to separate each trace for clarity.)

6.2 Statistical Prediction Models

6.2.1 Fall 2010 Results

Testing in the fall of 2010 took place on November 1st-11th, 2010 in Ames, Iowa at the Iowa State University Engineering Farm Bass field. During the harvest, the average corn yield was 137 bu/ac with an average grain moisture of 14%. The stover moisture ranged from 5.07 to 12.69 % moisture with an average moisture content of 8.7%. Stover flow rates ranged from 5.6 to 14 lb/s with an average mass-flow-rate of 8.15 lb/s.

Configuration testing of the dual axis chopper resulted in the plugging of the chopper during some high speed test runs. Poor feeding of the chopper caused the corn stover to build up inside the threshing area of the combine. Material then began to back up against the impact plate and rotor discharge beater. This resulted in spikes in the sensor responses because of material pressing against the impact plate. Test runs where this occurred were removed from analysis. Eight test runs were not affected by feeding problems from the chopper and were used for data analysis.

The design of experiments for the fall 2010 testing was constructed to determine the effects of combine ground speed and wet stover flow rate on the load cell force response of the stover impact plate. The wet stover flow rate was found to be significant with all the force components of the impact plate load cells. The vertical and horizontal were found to be most significantly correlated with the mass flow rate of the stover. The ground speed of the combine was not found to be significant with any of the force components of the impact plate load cells.

Prediction models of the mass flow rate were created using the sum of the horizontal load cell force responses, sum of the vertical load cell force responses, and the magnitude load cell force responses. As stated in the DOE results previously each force component produced a significant model by itself and the horizontal and vertical summed forces together produced a significant model. In 2010, stover moisture was not a significant factor and did not improve any of the force based flow rate prediction models.

Table 5: Stover flow rate prediction models created using the Fall 2010 data set.

Model #	Prediction Equation	Adjusted R^2	RMSE
1	$\dot{M}=3.464+\sum HF*1.582$	0.811	1.287
2	$\dot{M}=4.308+\sum VF*1.135$	0.821	1.253
3	$\dot{M}=-19.056+MF*2.479$	0.721	1.567
4	$\dot{M}=3.421+\sum HF*0.861+\sum VF*0.644$	0.911	0.885

Where:

$\dot{M}$= Wet Stover Mass Flow rate

$\sum HF$= The sum of the measured horizontal force components

$\sum VF$= The sum of the measured vertical force components

MF= The magnitude of the force components

Prediction Model 4 had an $R^2=0.911$ which means that the prediction equation can explain 91.1% of the variability in the data. Sources of unexplained variability may have come from noise in the load cell signals and inaccurate baseline calculations. Variability form the portions of stover falling from the rotor to the chaffer should be minimal because testing conditions did not greatly vary. Figure 11 shows the predicted stover mass-flow rates compared to actual mass-flow-rates for the best model created with the Fall 2010 data set. The data points follow the center line and all data points but one are within the confidence bands. The confidence bands in Figure 11 show where 95% of resulting intervals would capture the actual mean values if an infinite number of samples are taken.

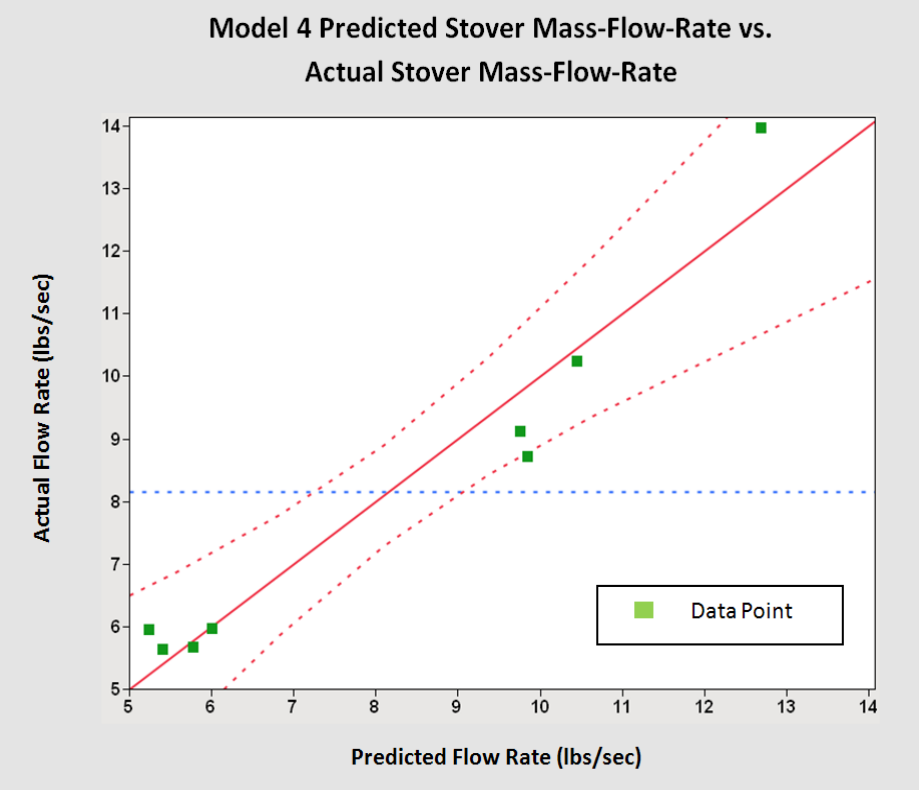

Figure 11: Predicted stover mass-flow-rate vs. actual stover mass-flow-rate (Wet Basis) the best prediction model for 2010 Fall Harvest.

Uncertainties of the prediction models were calculated by using Taylor Series Expansion. The uncertainty of Prediction Model 1 ranged from 1.919 to 5.370 lb/s with an average uncertainty of 3.472 lb/s. Prediction Model 2 had an uncertainty range of 1.230 to 4.337 lb/s with an average uncertainty of 2.605 lb/s. All the uncertainties of Prediction Model 3 were 0.375 lb/s. The uncertainties of Prediction Model 4 varied from 1.310 to 3.813 lb/s with an average uncertainty of 2.418 lb/s.

Results from the Fall 2010 testing showed that the impact plate sensor could be used to measure stover flow rate through the combine, that stover moisture was not significant in a mass flow prediction equation, and that the impact plate sensor was susceptible to noise created by the combine. Statistical analysis of the Fall 2010 data showed that the vertical, horizontal, and magnitude force components could be used to predict the mass flow rate of stover passing through the combine. Stover moisture was not found to be statistically

significant and this was most likely due to the lack of variability in stover moisture in the fall 2010 data set. It was also discovered that the impact plate was susceptible to noise causing an inaccurate baseline interval which caused inaccurate readings of sensor response. Another source of sensor noise was plugging of the rotor discharge beater caused large spikes in the load cell readings due to stover material wedging between the impact plate and discharge beater. The sensor response during test runs also contained a large amount of noise relative to the sensor response. After the Fall 2010 results were reviewed it was determined that the impact plate design was effective in measuring the flow rate for stover and that more testing was required to evaluate the effects of stover moisture.

6.2.2 Summer 2011 Results

Stover mass-flow-rates for the Summer 2011 data set ranged from 2.29 to 10 lb/s with an average flow rate of 5.5 lb/s. Stover moistures ranged from 6.25 to 24.6% with an average moisture of 15.7% and chopper speeds ranged from 1433 to 1472 rpm with an average of 1450 rpm. Wedging of stover between the rotor discharge beater and impact plate caused inaccurate and unusable data in ten test runs and these ten test runs were withheld from the statistical analysis. Seventeen of the twenty-seven test runs were used in the final statistical analysis.

The Summer 2011 design of experiments was constructed to evaluate the effects of wet stover flow rate, stover moisture, and stover feed rate with the measured response of the impact plate load cells. Wet stover flow rate was not found to be significant with the horizontal, vertical, or magnitude load cell force components. Stover moisture was also not found to be significant with any of the horizontal, vertical, or magnitude load cell force components. The vertical and magnitude load cell force components of the impact place load cells were not found to be significant with the stover feed rate into the combine. The horizontal load cell force response however, was found to be significant with the stover feed rate to the 0.0357 level.

A significant prediction model was created using the following prediction factors: Sum of horizontal forces, stover moisture, chopper speed, and stover moisture*chopper

speed. Stover moisture played a significant role in the prediction model and no statistically significant models could be produced without using stover moisture. This is expected as the moisture of the stover would affect the coefficient of restitution on the stover impacting the impact plate. The effects of using baled stover and stover baled from multiple fields also could have affected the test data. This may be one reason why statistically significant models containing few variables could not be created. Table 6 shows the prediction equation created using the Summer 2011 data.

Table 6: Stover flow rate prediction models created using the Summer 2011 data set.

Model #	Prediction Equation	Adjusted R^2	RMSE
5	$\dot{M}=190.921+\sum HF*35.898-SM*0.318-CS*0.125-CS*\sum HF*0.025$	0.893	0.801

Where:

SM= Stover Moisture

CS= Combine chopper speed

Stover moisture was most likely found to be significant because of the larger range in stover moistures. Stover moisture would affect the coefficient of restitution causing a different transfer of force from the stover to the impact plate as moisture varied. The speed of the combine chopper can be directly related to the discharge beater speed of the combine. The varied speed of the discharge beater would cause the stover to contact the impact plate at different speeds causing a varied load cell response. The significance of the chopper speed could have also been related to the threshing load of the combine. An increase in flow rate through the combine would have caused the threshing speed of the combine to slow.

Prediction model 5 had an R^2=0.893 implying that the prediction model could explain 89.3% of the variability in the prediction model. Sources of unexplained variability may have come from an inaccurate baseline interval and from the portion of stover falling on the

chaffer of the combine and not being expelled by the discharge beater against the impact plate. These portions may have been different depending on the stover bales and TMR unloading time. The stover bales used for testing may have contained different stover particle sizes resulting in different amounts of stover falling onto the chaffer. Also the unloading time of the TMR mixer may have affected the stover particle size. Greater unloading time would result in more processing of the stover and a smaller particle size of the stover.

Figure 12 shows the predicted stover mass-flow-rate compared to the actual stover mass-flow rate for the Summer 2011 data. The high moisture level data is located towards the lower end of the flow rates. The mid moisture data points are also located in the lower range of flow rates. During high flow rate test runs of the mid moisture stover, wedging of the stover between the impact plate and discharge beater was experienced and that is why there are few data points from this moisture level. Flow rates during the low moisture test runs were greater because the combine capacity for dry stover was greater. Also high flow rate test runs with dry stover did not result in wedging between the impact plate and rotor discharge beater. The variation in flow rates of the different moisture levels was due to the capacity and capability of the combine to process stover of different moisture levels.

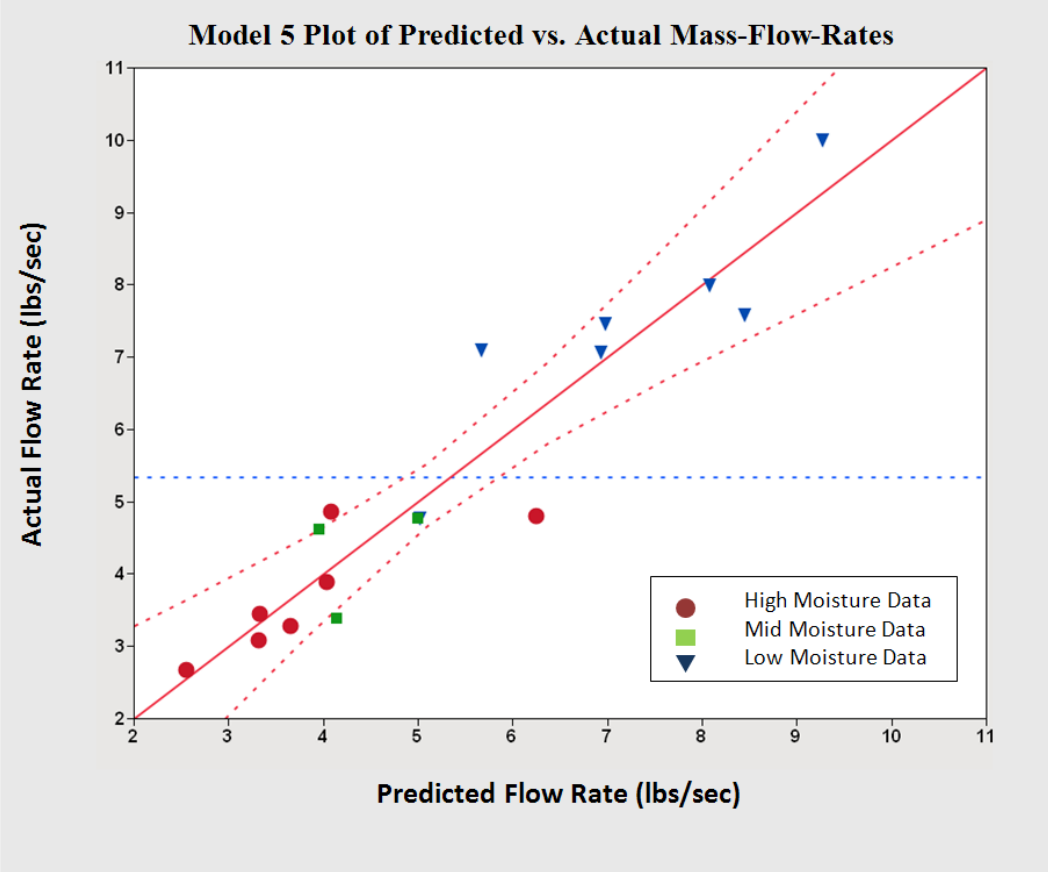

Figure 12: Predicted mass-flow-rate of stover compared to actual stover mass-flow-rate (Wet Basis) with confidence bands for prediction model 5

Results from the Summer 2011 testing showed that the horizontal load cell could be used to predict the mass flow of stover through the combine along with stover moisture and the combine chopper speed. The sum of the horizontal forces from the load cells was also shown to be significant in predicting the stover flow rate during Fall 2010 testing. Stover moisture and combine chopper speed were not found to be significant in previous testing.

6.2.3 Fall 2011 Results

Testing in the fall of 2011 took place between October 3rd and November 19th with high moisture tests run October 3rd-5th, mid moisture tests run October 20th-24th, and low

moisture tests run November 18th-19th. Stover moistures ranged from 13 to 52% with an average moisture content of 17.2%. Grain moistures averaged 18.3% moisture for the high moisture tests, 15% moisture for the mid moisture tests, and 14.3% moisture for the low moisture tests. Stover flow rates ranged from 7.3 to 17.5 lb/s with an average flow rate of 10.6 lb/s. During the high moisture repetition, the 4 mph ground speed could not be obtained because the combine did not have adequate engine power and capacity to run at this higher ground speed; therefore, only the low speed tests were conducted during the high moisture treatment. During six of the thirty-six test runs, stover became wedged between the rotor discharge beater and impact plate causing inaccurate sensor readings. The six affected data sets were withheld from statistical analysis.

The DOE interactions between the sensor responses and test variables were examined to determine if the variables affected the sensor response. The wet stover flow rate was found to be statistically significant with the horizontal sum of forces and magnitude forces of the load cell responses. The wet stover flow rate was not significant with the vertical sum of forces. The stover moisture was statistically significant with the vertical and magnitude force responses of the load cells. However, stover moisture was not statistically significant with the horizontal forces of the load cell responses. The ground speed of the combine was statistically significant with all force components of the load cell response. The head height was found to be significant with the horizontal force component of the load cells, but not with the vertical and magnitude force components of the load cells.

Statistical analysis of the processed data showed that component forces measured by the impact plate load cells were significantly correlated to the stover mass-flow-rate. Prediction models created with the Fall 2011 data set are presented in Table 7. The horizontal sum of the component forces and magnitude of forces produced statistically significant prediction models (alpha = 0.05). In Table 7, Model 6 and Model 7 present the prediction equations using the sum of the horizontal forces and the magnitude of the forces respectively. Adding the stover moisture to a prediction model using the sum of the horizontal forces increased the adjusted R^2 and reduced the RSME of the prediction model from 0.324 and 2.752 to 0.709 and 1.805 respectively. Adding the stover moisture to a

prediction model using the magnitude of forces increased the adjusted R^2 and reduced the RSME of the prediction model from 0.599 and 2.118 to 0.785 and 1.550 respectively. The increase in the accuracy of the prediction models including stover moisture shoes the important role of this variable has on the impact force response measured by the load cells. Model 10 in Table 7 uses the magnitude of the forces, stover moisture, and chopper speed as well as interactions between stover moisture *chopper speed and chopper speed*magnitude of forces produced a prediction model with a much higher adjusted correlation coefficient, 0.909 and lower RMSE, 1.009 than any other Fall 2011 prediction model. The ground speed of the combine and head height did not add to the significance of any of the prediction models.

Table 7: Stover flow rate prediction models created using the Fall 2011 data set.

Model #	Prediction Equation	Adjusted R^2	RMSE
6	$\dot{M}$=4.153-∑HF*1.305	0.324	2.752
7	$\dot{M}$=-9.017+MF*3.370	0.599	2.118
8	$\dot{M}$=1.370-∑HF*0.956+ SM*0.215	0.709	1.805
9	$\dot{M}$=-6.805+MF*2.405+ SM*0.164	0.785	1.550
10	$\dot{M}$=-187.050+MF*49.805-SM*4.058+CS*0.132+ SM*CS*0.003-CS*MF*0.035	0.909	1.009

Examining to coefficients of the variables in the prediction equations explains how each variable affects the prediction equation. Prediction models 6 and 7 show that as the measured impact force increase the predicted stover flow rate increase. The effect of the stover force on predicted flow rate is expected as high flow rates should lead to an increase in the measured forces. The effects of the load cells force from models 6 and 7 are repeated in models 8 and 9, but the coefficient of stover moisture shows that as stover moisture increases

the predicted flow rate increases. This is expected as the increases in stover moisture would increase the mass of the stover if the dry flow rate of stover remained the same. Examining the effect of chopper speed in prediction model 10 shows that an increase in chopper speed results in a decrease in predicted stover flow rate. This is due to the size of the coefficient in the interaction between chopper speed and the sum of the magnitude forces.

Prediction model 10 was the best model created using the Fall 2011 test data and the model had an R^2=0.909 implying that the prediction model could explain 90.9% of the variability in the data. Sources of unexplained data variability may have come from inaccurate baseline intervals or the chaffer and rotor portions of the stover. The variability form the chaffer and rotor portions of stover however should be minimal, because the moisture of the stover in the prediction model should explain this. Stover moisture should explain crop maturity and in return explain the portion stover falling onto the chaffer.

Uncertainties of the Fall 2011 prediction models were calculated using Taylor Series Expansion of the prediction models. Prediction Model 6 had an uncertainty range of 1.678 to 5.374 lb/s with an average uncertainty of 3.712 lb/s. Prediction Model 7 had an uncertainty range of 0.278 to 0.540 lb/s with an average uncertainty of 0.489 lb/s. Prediction Model 8 had an uncertainty range of 1.240 to 3.967 lb/s with an average uncertainty of 2.722 lb/s. Prediction Model 9 had an uncertainty range of 0.234 to 0.385 lb/s with an average uncertainty of 0.359 lb/s. Uncertainty of Prediction Model 10 ranged from 0.059 to 0.648 lb/s with an average uncertainty of 0.259 lb/s.

The predicted stover mass-flow-rates verse the actual stover mass-flow-rate for Prediction Model 10 is shown in Figure 13. The high moisture data was grouped towards the high end of the actual flow rates. This is a result of moisture content of the stover adding to the weight of the stover. The difference in high moisture flow rates of the Summer 2011 testing data and Fall 2011 testing data may be due to the artificial increase in stover moisture and actual stover moisture. The mid moisture data was scattered along most of the flow-rate

range. Low moisture mass flow rates were concentrated towards the lower end of the mass-flow-rates.

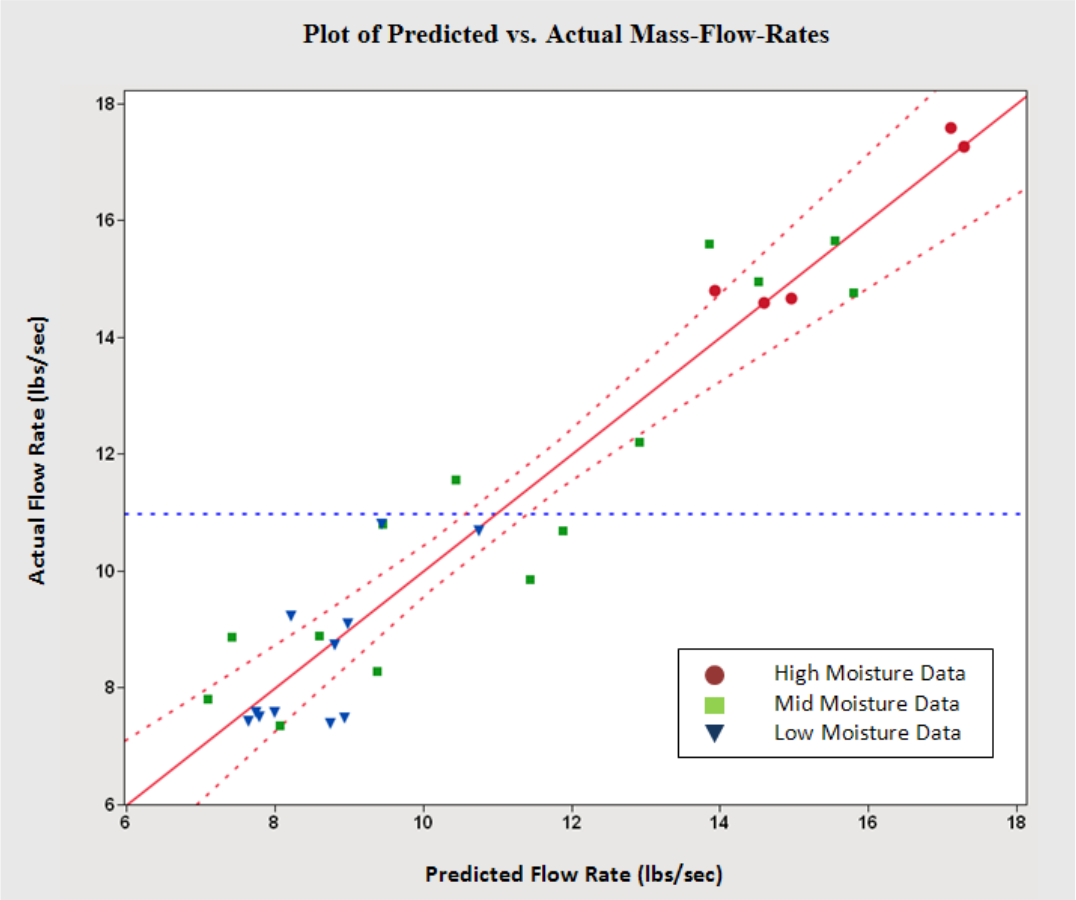

Figure 13: Predicted mass-flow-rate of stover compared to actual stover mass-flow-rate (Wet Basis) for Prediction Model 10.

Results from Fall 2011 testing showed that the impact plate mass flow sensor could be used in a variety of conditions to measure the mass flow rate of stover through the combine. The horizontal and vertical force components measure by the impact plate alone were able to measure the mass flow rate of stover with reasonable success, but when the stover moisture was utilized the accuracy of the prediction equation accuracy increased greatly.

CHAPTER 7.0 CONCLUSIONS AND RECOMMENDATIONS

7.1 Conclusions

The objective of this research was to determine if stover mass-flow-rate through a combine could be measured with an impact plate located behind the rotor discharge beater. To validate this objective a curved steel impact plate was installed behind the rotor discharge beater and six load cells were used to record the impact forces acting on a curved plate located behind the rotor discharge beater by the stover. The following conclusions were made about the use of an impact plate to measure stover mass-flow-rate though the combine:

1. Force components of load cells connected to the impact plate could be used to predict stover mass-flow-rate through the combine.
2. Stover moisture and chopper speed were found to be significant prediction factors in the Summer 2011 and Fall 2011 test sets. Cut height did not have an effect on sensor response during the Fall 2011 tests.
3. Responses of the load cell contained a large amount of noise.
4. The reading of the load cells was relatively small compared to the full scale capacity of the load cells. This resulted in a large amount of uncertainty from the load cell prediction component to the models.
5. An inaccurate baseline interval greatly affects the accuracy of the prediction equation.
6. The best fall 2011 prediction model could predict the stover mass-flow-rate within $\pm$1.09 lb/s. This was 6-15% error depending on the flow rate.
7. Wear patterns in the paint on the impact plate suggest that most material contacts the impact plate between location 2 and 7. Figure 14 shows the impact plate after Fall

2011 testing. Some paint still remains at the impact point 1 location suggesting that this area of the impact plate does not receive large amounts of stover contact.

Figure 14: Image of impact plate taken after Fall 2011 harvest showing wear patterns in paint caused by impacting stover.

7.1 Future Recommendations

Initial evaluation and testing of the impact plate sensor produced results that suggest future work should be conducted to improve the impact plate sensor effectiveness at measuring stover mass flow rate.

1. Signals from the load cells contained large amounts of cyclical noise. The rotor discharge beater contains ten paddles and rotates at 1000 rpm. Using this observation a dominate pulse frequency should be seen at 166 Hz. FFT analysis of the Fall 2010 data showed that there was a dominate signal in the 166 to 185 Hz range. Future analysis should be conducted to examine if filtering data about these frequencies would produce a more accurate prediction equation.
2. An alternate method should be developed to determine the baseline interval of the load cells. An inaccurate baseline interval greatly affected the accuracy of the prediction models. Current methods used in combine grain yield monitors could be applied to the impact plate sensors to develop a more robust baseline calibration.
3. Changes should be made to reduce the uncertainty of the mass flow prediction equation. The easiest way to accomplish this would be to use a load cell that uses its entire full scale range when measuring the forces.

WORKS CITED

Andrews, S. S. 2006. Crop Residue Removal for Biomass Energy Production: Effects on Soil and Recommendations. Available at http://soils.usda.gov/sqi/management/files/AgForum_Residue_White_Paper.pdf (accessed 24Jan. 2012) USDA-Natural Resources Conservation Service.

Chaplin, J., N. Hemming, B. Hetchler. 2003. Comparison of an impact plate and torque based yield sensors. ASAE Paper No. 031034. St Joseph, Mich.: ASAE.

Deere & Company. 2012. John Deere HarvestLab™ Now Provides More Nutrient Analysis of Silage [Press release]. Available at http://www.deere.com/wps/dcom/en_US/corporate/our_company/news_and_media/press_releases/2012/agriculture/2012jun29_harvestlab.page. Accessed 12Feburary. 2013.

Havorson, A. D., G. A. Peterson and C. A. Reule. 2002 Tillage Systems and Crop Rotation Effects on Dryland Crop Yields and Carbon in the Central Great Plains. *Agronomy Journal.* 1429-1436

History Timeline 1992. AG Leader Technology, Ames, IA. Available at http://www.agleader.com/includes/history/1992.html. Accessed 12Febuary. 2013.

Ag Leader. History Timeline 1992. AG Leader Technology, Ames, IA. Available at http://www.agleader.com/includes/history/1992.html. Accessed 12Febuary. 2013.

Johnson, J. M. -F., R. R. Allmaras and D. C. Reicosky. 2006. Estimating Source Carbon from Crop Residues, Roots and Rhizodeposits Using the National Grain-Yield Database. American Society of Agronomy. 622-636

Linden, D. R., C. E. Clapp and R. H. Dowdy. 2000. Long-Term Corn Grain and Stover Yields and a Function of Tillage and Residue Removal in East Central Minnesota. Soil and Tillage *Research.* 56: 167-174

Martel. H. and P. Savonie. 2000. Sensors to Measure Mass-Flow-Rate Through a Forage Harvester. *Canadian Agricultural Engineering*. 42(3): 123-129

NASS. 2011. Acreage. Washington, D.C.: National Agricultural Statistics Service, U.S. Department of Agriculture.

Oak Ridge National Laboratory. 2005. Biomass as Feedstock for a Bioenergy and Bioproducts Industry: The Technical Feasibility of a Billion-Ton Annual Supply. Oak Ridge: U.S. Department of Energy, U.S. Department of Agriculture.

Pfeiffer, D. W., J. W Hummel, and N. R. Miller. 1993. Real-time corn yield sensor. ASAE Paper No. 931013. St Joseph, Mich.: ASAE.

Prince, S. D.,J. Hassket, M. Steininger, H Strand and R. Wright. 2001. Net Primary Production of U.S. Midwest Croplands From agricultural Harvest Yield Data. *Ecological Applications*. 11(4).: 1194-1205.

Savoie, P. P. Lemire and R. Theriault. 2002. Evaluation of Five Sensors to Estimate Mass-Flow Rate and Moisture of Grass in a Forage Harvester. Applied Engineering in Agriculture. 18(4): 389-397.

Sensoray. 2001. Sensoray Model 518 PCbus Sensor Coprocessor. Sensoray, Tigard, OR. Available at http://www.sensoray.com/downloads/518manual.PDF. Accessed 4May. 2011.

Shinners, K. J., N. G. Barnett., and W. M. Schlesser. 2000. Measuring mass-flow-rate on forage
cutting equipment. ASAE Paper No. 001036. St. Joseph, Mich.: ASAE
Shinners, K. J., B. M. Huenink and C. B. Behringer. 2003. Precision Agriculture as Applied to
North American Hay and Forage Production. In Electronic Proceedings of the International Conference on Crop Harvesting and Processing, ASAE.

Veal, M., S. Shearer, and J. Fulton. 2004. Improve Flow Sensing for Yield Monitoring in Grain Combines. ASABE Paper No. 041101. St. Joseph, MI.: ASABE

Wilhelm, W., J. Johnson, D. Karlen, and D. Lightle. 2007. Corn Stover to Sustain Soil Organic Carbon Further Constrains Biomass Supply. Agronomy Journal. 99: 1665-1667

USDA-ARS. 2003. Draft User's Guide Revised Universal Soil Loss Equation Version 2 (RUSLE2). Available at http://fargo.nserl.purdue.edu/rusle2_dataweb/RUSLE2_Index.htm (accessed 24Jan. 2012) USDA-ARS, Washington, DC.

Yield Monitor 2000 Operators Manual. AG Leader Technology, Ames IA. Available at http://www.agleader.com/docs/manual-ym2k-jun99.pdf. Accessed 12Febuary. 2010.

APPENDIX A: Detailed Equations to Determine Stover Impact Forces

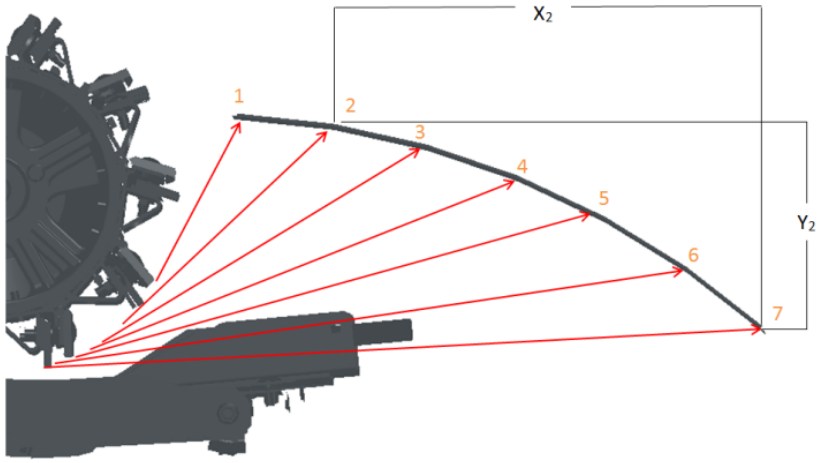

Figure 15: Diagram of impact plate showing impact vectors, analyzed impact locations, and referenced dimensions of impact locations.

Impact calculations for impact point 2 began by taking a moment about point 7.

Equation 8: $$M_7 = 0 = F_1\left(\sqrt{X_1^2 + Y_1^2}\right) - F_{2Y}(X_2) - F_{2X}(Y_2)$$

Where:

M_7= a moment at impact point 7

F_1= the measured force response at point 1

$\sqrt{X_1^2 + Y_1^2}$= the calculated distance between impact point 1 and impact point 7

F_{2Y}= the vertical force at impact point 2

X_2= the horizontal distance between impact point 2 and impact point 7

F_{2X}= the horizontal force at impact point 2

Y_2= the vertical distance between impact point 2 and impact point 7

The resultant force F_1 can now be solved for. Then the horizontal and vertical forces can be summed.

Equation 9: $\sum F_Y = 0 = -F_{1Y} + F_{2Y} - F_{7Y}$

Equation 10: $\sum F_X = 0 = -F_{1X} + F_{2X} - F_{7X}$

Where:

$\sum F_Y$ = the sum of the vertical force components

F_{1Y} = the vertical force component of resultant force 1

F_{2Y} = the vertical force component of the relative impact force and impact point 2

F_{7Y} = the vertical force component of resultant force 7

$\sum F_X$ = the sum of the horizontal force components

F_{1X} = the horizontal force component of resultant force 1

F_{2X} = the horizontal force component of the relative impact force and impact point 2

F_{7X} = the horizontal force component of resultant force 7

Modifying for each impact location Equation 8, Equation 9, and Equation 10 can be used to solve the measured force responses at all impact points.

APPENDIX B: Test Data from Fall 2010, Summer 2011, and Fall 2011 test repetitions

Table 8: Fall 2010 Test Data

Run Number	Stover Flow Rate (lb/s)	Stover Moisture (%)	Chopper Speed (RPM)	Sum of Horizontal Forces (lb)	Sum of Vertical Forces (lb)	Magnitude of Forces (lb)
1	5.627	7.738	1440	1.314	1.336	10.349
2	9.116	8.403	1396	2.678	6.272	12.269
3	5.965	12.694	1445	2.227	1.046	9.935
4	5.662	5.065	1454	1.597	1.534	10.062
5	8.712	12.107	1438	4.465	4.021	11.096
6	5.947	7.195	1452	1.154	1.287	9.924
7	13.957	10.354	1388	5.598	6.921	12.171
8	10.241	10.654	1391	4.673	4.678	12.017

Table 9: Summer 2011 Test Data

Run Number	Moisture level	Stover Flow Rate Level	Stover Flow Rate (lb/s)	Stover Moisture (%)	Chopper Speed (RPM)	Sum of Horizontal Forces (lb)	Sum of Vertical Forces (lb)	Magnitude of Forces (lb)
1	High	Mid	3.893	16.319	1460	-0.357	-1.195	4.279
2	Low	Mid	7.993	9.269	1445	-2.258	-3.079	5.279
3	Low	High	10.003	7.462	1435	-2.528	-1.101	4.649
4	Low	Low	7.586	8.035	1445	-1.835	-1.389	4.561
6	Low	High	7.089	15.315	1452	-2.191	-1.733	5.099
7	Low	Mid	7.458	11.363	1448	0.762	11.679	11.371
8	Low	Low	4.774	15.55	1453	0.025	1.474	8.495
9	Mid	High	3.275	24.621	1454	-7.079	-5.107	8.953
10	High	Low	3.080	22.3176	1452	-1.773	-1.319	6.119
11	High	Mid	2.671	23.958	1458	-2.491	-0.340	6.207
12	High	Mid	4.794	14.666	1443	-6.722	1.073	13.222
14	High	Low	3.450	19.658	1464	-1.953	-0.398	4.741
15	High	Mid	4.862	19.658	1459	-3.071	-2.249	5.302
16	Low	High	7.060	10.256	1454	-1.533	0.881	5.036
17	Mid	High	4.617	19.2486	1439	-11.409	-13.292	11.983
18	Mid	Low	3.380	16.216	1457	0.865	0.629	5.005
19	Mid	Mid	4.766	18.859	1447	-4.589	-5.507	8.287

Table 10: Fall 2011 Test Data

Run Number	Moisture level	Ground Speed Level	Head Height Level	Stover Flow Rate (lb/s)	Stover Moisture (%)	Chopper Speed (RPM)	Sum of Horizontal Forces (lb)	Sum of Vertical Forces (lb)	Magnitude of Forces (lb)
1	High	Low	Low	14.798	34.31	1380	-5.084	-1.629	6.260
2	High	Low	High	14.592	36.61	1404	-4.840	-1.875	5.706
3	High	Low	High	17.252	43.09	1374	-7.009	-1.822	7.120
4	High	Low	Low	17.569	51.92	1341	-6.195	-2.326	6.961
5	High	Low	Low	14.666	38.27	1378	-6.132	-1.852	6.380
6	Mid	Low	High	7.796	13.55	1429	-4.433	-0.576	5.435
7	Mid	High	Low	9.856	20.69	1351	-5.883	-3.029	6.240
8	Mid	High	Hgih	14.758	21.1	1301	-6.735	-4.216	6.971
9	Mid	Low	Low	8.281	19.66	1414	-4.306	-3.353	5.523
10	Mid	High	High	12.203	17.65	1349	-6.587	-3.443	6.870
11	Mid	High	Low	14.946	17.2	1299	-5.884	-4.492	6.651
12	Mid	Low	High	8.853	14.29	1436	-4.197	-2.388	4.765
13	Mid	High	High	15.585	13.25	1319	-7.234	-2.603	6.745
14	Mid	Low	High	10.796	20.67	1405	-4.019	-2.542	5.268
15	Mid	Low	Low	15.640	34.44	1359	-6.546	-2.835	7.080
16	Mid	High	High	11.549	17.22	1355	-5.792	-2.597	6.075
17	Mid	Low	High	7.337	16.28	1428	-2.376	-2.085	4.777
18	Mid	Low	Low	8.888	18.18	1422	-4.128	-2.214	4.649
19	Mid	High	Low	10.679	19.31	1361	-4.223	-2.276	6.604
20	High	Low	High	7.579	14.58	1417	-3.572	-4.908	5.672
21	High	Low	High	7.500	15.63	1434	-5.738	-4.500	5.742
22	High	High	High	10.676	14.74	1367	-7.261	-5.996	6.567
23	High	Low	Low	7.418	15.12	1418	-3.351	-4.095	5.052
24	High	High	Low	9.093	16.16	1366	-6.047	-3.405	5.642
25	High	Low	High	7.568	16.67	1419	-2.654	-2.697	4.621
26	High	High	Low	7.478	16.22	1386	-6.099	-3.751	5.788
27	High	Low	Low	7.384	18.18	1425	-2.574	-3.633	4.989
28	High	High	High	8.723	16.88	1411	-6.930	-4.674	5.982
29	High	High	Low	9.213	16.07	1408	-3.729	-4.660	5.449
30	High	High	Low	10.794	15.38	1393	-7.405	-4.818	6.440

APPENDIX C: Uncertainty Analysis

Moisture Uncertainty Analysis

Sample moisture was calculated on a wet moisture basis. Equation 11 shows the wet basis moisture calculation.

$$\textbf{Equation 11: } \boldsymbol{Percent\ Moisture} = \frac{W-D}{W} * 100$$

Where:

W = the wet moisture sample weight

D = the dry moisture sample weight

To calculate the uncertainty of the sample moisture sample Taylor Series Expansion was utilized. Equation 12 shows the uncertainty expansion of the wet basis moisture calculation.

$$\textbf{Equation 12: } \Delta E = \left[\left(\frac{\partial E}{\partial W}\Delta W\right)^2 + \left(\frac{\partial E}{\partial D}\Delta D\right)^2\right]^{\frac{1}{2}}$$

Where:

ΔE= the total uncertainty in the moisture calculation

$\frac{\partial E}{\partial W}$= the partial derivative with respect to the wet weight measurement

ΔW= the uncertainty in the wet weight measurement

$\frac{\partial E}{\partial D}$= the partial derivative with respect to the dry weight measurement

ΔD= the uncertainty in the dry weight measurement

Equation 13 shows the results from the partial derivative and Equation 13 was used to calculate the uncertainty of the sample moistures.

Equation 13: $\Delta E = \left[\left(\frac{1}{W^2}\Delta W\right)^2 + \left(\frac{-1}{W^2}\Delta D\right)^2\right]^{\frac{1}{2}}$

The uncertainty in both the wet weight and dry weight was 0.02 kg. For the Fall 2010 sample moistures additional equations needed to be developed. Equation 14 was used to calculate the moisture for each test run.

Equation 14: $Run\ Moisture = \frac{M_a + M_b}{2}$

Where:

M_a= the moisture calculated for sample a

M_b= the moisture calculated for sample b

To calculate the uncertainty in the average Taylor Series Expansion of Equation 14 was used. Equation 15 shows the partial derivatives of Equation 14.

Equation 15: $\Delta E = \left[\left(\frac{\partial E}{\partial M_a}\Delta M_a\right)^2 + \left(\frac{\partial E}{\partial M_a}\Delta M_b\right)^2\right]^{\frac{1}{2}}$

Where:

$\frac{\partial E}{\partial M_a}$= the partial derivative of Equation 14 with respect to M_a

ΔM_a= the uncertainty in M_a stover moisture

$\frac{\partial E}{\partial M_b}$= the partial derivative of Equation 14 with respect to M_b

ΔM_b= the uncertainty in M_b stover moisture

Equation 15 results in Equation 16 which can be used to calculate the uncertainty in the Fall 2010 stover moisture for each test run.

Equation 16: $\Delta E = \left[\left(\frac{M_a}{4}\Delta M_a\right)^2 + \left(\frac{M_b}{4}\Delta M_b\right)^2\right]^{\frac{1}{2}}$

Moisture uncertainties for all data test sets are shown in Tables 11, 12, and 13.

Table 11: Fall 2010 Moisture Uncertainty

Run #	Sample	Wet Weight (Kg)	Dry Weight (Kg)	Sample Stover Moisture	Measurement Uncertainty (Kg)	Sample Moisture Uncertainty (% Moisture)	Stover Moisture	Moisture Uncertainty (% Moisture)
1	a	0.56	0.516	7.86%	0.02	9.85%	8.33%	0.24%
	b	0.63	0.582	7.62%	0.02	7.76%		
2	a	0.67	0.611	8.81%	0.02	6.97%	10.39%	0.20%
	b	0.7	0.644	8.00%	0.02	6.32%		
3	a	0.66	0.581	11.97%	0.02	7.50%	6.97%	0.29%
	b	0.79	0.684	13.42%	0.02	5.34%		
4	a	0.86	0.843	1.98%	0.02	3.90%	6.98%	0.08%
	b	0.92	0.845	8.15%	0.02	3.66%		
5	a	0.684	0.602	11.99%	0.02	6.98%	7.98%	0.26%
	b	0.818	0.718	12.22%	0.02	4.90%		
6	a	0.829	0.796	3.98%	0.02	4.29%	7.26%	0.15%
	b	0.759	0.68	10.41%	0.02	5.55%		
7	a	0.768	0.687	10.55%	0.02	5.43%	10.66%	0.20%
	b	0.748	0.672	10.16%	0.02	5.69%		
8	a	0.938	0.837	10.77%	0.02	3.65%	5.38%	0.17%
	b	0.797	0.713	10.54%	0.02	5.04%		

Table 12: Summer 2011 Moisture Uncertainty

Run #	Wet Weight (Kg)	Dry Weight (Kg)	Stover Moisture (%)	Measurement Uncertainty (kg)	Moisture Uncertainty (% Moisture)
1	2.88	2.41	16.32%	0.02	0.42%
2	3.56	3.23	9.27%	0.02	0.25%
3	2.68	2.48	7.46%	0.02	0.43%
4	3.36	3.09	8.04%	0.02	0.27%
5	2.22	1.88	15.32%	0.02	0.70%
6	2.64	2.34	11.36%	0.02	0.46%
7	3.6	3.04	15.56%	0.02	0.27%
8	5.28	3.98	24.62%	0.02	0.15%
9	4.66	3.62	22.32%	0.02	0.18%
10	3.84	2.92	23.96%	0.02	0.27%
11	4.5	3.84	14.67%	0.02	0.17%
12	4.68	3.76	19.66%	0.02	0.17%
13	4.68	3.76	19.66%	0.02	0.17%
14	4.68	4.2	10.26%	0.02	0.15%
15	4.78	3.86	19.25%	0.02	0.16%
16	5.18	4.34	16.22%	0.02	0.13%
17	4.56	3.7	18.86%	0.02	0.17%

Table 13: Fall 2011 Moisture Uncertainty

Run #	Wet Weight (Kg)	Dry Weight (Kg)	Stover Moisture (%)	Measurement Uncertainty (Kg)	Moisture Uncertainty (% Moisture)
1	5.48	3.6	34.31%	0.02	0.09%
2	5.08	3.22	36.61%	0.02	0.11%
3	5.31	3.02	43.09%	0.02	0.10%
4	8.53	4.1	51.92%	0.02	0.04%
5	5.54	3.42	38.27%	0.02	0.09%
6	3.1	2.68	13.55%	0.02	0.29%
7	3.48	2.76	20.69%	0.02	0.23%
8	4.36	3.44	21.10%	0.02	0.15%
9	3.56	2.86	19.66%	0.02	0.22%
10	3.4	2.8	17.65%	0.02	0.24%
11	3.72	3.08	17.20%	0.02	0.20%
12	3.36	2.88	14.29%	0.02	0.25%
13	3.32	2.88	13.25%	0.02	0.26%
14	3.58	2.84	20.67%	0.02	0.22%
15	4.82	3.16	34.44%	0.02	0.12%
16	3.02	2.5	17.22%	0.02	0.31%
17	2.58	2.16	16.28%	0.02	0.42%
18	3.08	2.52	18.18%	0.02	0.30%
19	2.9	2.34	19.31%	0.02	0.34%
20	1.92	1.64	14.58%	0.02	0.77%
21	1.92	1.62	15.63%	0.02	0.77%
22	1.9	1.62	14.74%	0.02	0.78%
23	1.72	1.46	15.12%	0.02	0.96%
24	1.98	1.66	16.16%	0.02	0.72%
25	1.92	1.6	16.67%	0.02	0.77%
26	2.22	1.86	16.22%	0.02	0.57%
27	2.2	1.8	18.18%	0.02	0.58%
28	1.54	1.28	16.88%	0.02	1.19%
29	2.24	1.88	16.07%	0.02	0.56%
30	1.82	1.54	15.38%	0.02	0.85%

Chopper Speed Uncertainty Analysis

Chopper speed was calculated by the data acquisition. The data acquisition system used the pulses from the slip ring (Michigan Scientific, Charlevoix MI) between data time stamps. Equation 17 shows the basic equation to calculate the chopper speed.

Equation 17: $\frac{Pulses}{Time\ Step}$

Taylor Series Expansion was conducted for each variable is shown in Equation 18.

Equation 18: $\Delta E = \left[\left(\frac{\partial E}{\partial P}\Delta P\right)^2 + \left(\frac{\partial E}{\partial T}\Delta T\right)^2\right]^{\frac{1}{2}}$

Where:

$\frac{\partial E}{\partial P}$= the partial derivative of the chopper speed equation for pulses

ΔP= the uncertainty in the pulse count

$\frac{\partial E}{\partial T}$= the partial derivative of the chopper speed equation for the time step

ΔT= the uncertainty in the time step

The uncertainty in the number of pulses per time step is shown in equation 19. The uncertainty in the number of pules is one pulse. The uncertainty of the Athena II time clock was not available from the manufacture so an uncertainty of 2% was assumed. To convert the pulses per count to RPM the conversion factor 1.17 needed to be used. This conversion factor was calculated using

Equation 20. The total uncertainty in the chopper speed measurement was 1.17 RPM.

Equation 19: $\Delta E = \left[\left(\frac{1}{P^2}\Delta P\right)^2 + \left(\frac{-1}{T^2}\Delta T\right)^2\right]^{\frac{1}{2}}$

Equation 20: $\frac{1\ pulse}{Time\ step} * \frac{Time\ step}{0.1\ second} * \frac{1\ revolution}{512\ pulses} * \frac{60\ seconds}{1\ minute} = 1.17\ \frac{revolutions}{minute}$

Load Cell Uncertainty Analysis

To calculate the uncertainty in the load cell measurement Taylor Series Expansion was conducted for the sum of the horizontal, sum of the vertical, and magnitude of the forces variables. Equation 21 was used to calculate the sum of the horizontal forces. Note that the sum of the vertical forces would be the same for that reason the sum of vertical forces uncertainty calculation was not shown.

Equation 21: $\sum F_X = X_1 + X_2 + X_3 + X_4 + X_5 + X_6$

Where:

$\sum F_X$ = the sum of the horizontal forces

X_1 = the horizontal force from load cell number 1

X_2 = the horizontal force from load cell number 2

X_3 = the horizontal force from load cell number 3

X_4 = the horizontal force from load cell number 4

X_5 = the horizontal force from load cell number 5

X_6 = the horizontal force from load cell number 5

The partial derivative of each horizontal force component was then calculated and is shown in Equation 22.

Equation 22: $\Delta F_x = \left[\left(\frac{\partial F_X}{\partial X_1}\Delta X_1\right)^2 + \left(\frac{\partial F_X}{\partial X_2}\Delta X_2\right)^2 + \left(\frac{\partial F_X}{\partial X_3}\Delta X_3\right)^2 + \left(\frac{\partial F_X}{\partial X_4}\Delta X_4\right)^2 + \left(\frac{\partial F_X}{\partial X_5}\Delta X_5\right)^2 + \left(\frac{\partial F_X}{\partial X_6}\Delta X_6\right)^2\right]^{\frac{1}{2}}$

Where:

ΔF_x = the uncertainty in the horizontal force measurement

$\frac{\partial F_X}{\partial X_1}$ = the partial derivative of Equation 18 with respect to F_{X1}

ΔX_1= the uncertainty in the horizontal force of load cell 1

$\frac{\partial F_X}{\partial X_2}$= the partial derivative of Equation 18 with respect to F_{X2}

ΔX_2= the uncertainty in the horizontal force of load cell 2

$\frac{\partial F_X}{\partial X_3}$= the partial derivative of Equation 18 with respect to F_{X3}

ΔX_3= the uncertainty in the horizontal force of load cell 3

$\frac{\partial F_X}{\partial X_4}$= the partial derivative of Equation 18 with respect to F_{X4}

ΔX_4= the uncertainty in the horizontal force of load cell 4

$\frac{\partial F_X}{\partial X_5}$= the partial derivative of Equation 18 with respect to F_{X5}

ΔX_5= the uncertainty in the horizontal force of load cell 5

$\frac{\partial F_X}{\partial X_6}$= the partial derivative of Equation 18 with respect to F_{X6}

ΔX_6= the uncertainty in the horizontal force of load cell 6

Equation 22 becomes Equation 23.

Equation 23: $\Delta F_x = [(X_1 * \Delta X_1)^2 + (X_2 * \Delta X_2)^2 + (X_3 * \Delta X_3)^2 + (X_4 * \Delta X_4)^2 + (X_5 * \Delta X_5)^2 + (X_6 * \Delta X_6)^2]^{\frac{1}{2}}$

The non-repeatability of the load cell was listed as 0.05% of the full scale range of the load cell. The MLP-300 load cell has a full scale range of 300 lb, resulting in a non-repeatability of 0.15 lb for each load cell.

Equation 24 shows how the magnitude of forces was calculated.

Equation 24: $Mf = (F_1^2 + F_2^2 + F_3^2 + F_4^2 + F_5^2 + F_6^2)^{1/2}$

Where:

Mf= the magnitude of the forces

F_1= the force measured by load cell 1

F_2= the force measured by load cell 2

F_3= the force measured by load cell 3

F_4 = the force measured by load cell 4

F_5 = the force measured by load cell 5

F_6 = the force measured by load cell 6

Taking the partial derivative with respect to each load cell force produced Equation 25.

Equation 25: $$\Delta MF = \left[\left(\frac{\partial F}{\partial F_1}\Delta F_1\right)^2 + \left(\frac{\partial F}{\partial F_2}\Delta F_2\right)^2 + \left(\frac{\partial F}{\partial F_3}\Delta F_3\right)^2 + \left(\frac{\partial F}{\partial F_4}\Delta F_4\right)^2 + \left(\frac{\partial F}{\partial F_5}\Delta F_5\right)^2 + \left(\frac{\partial F}{\partial F_6}\Delta XF_6\right)^2\right]^{\frac{1}{2}}$$

Where:

ΔMF = the uncertainty on the magnitude of the forces measurement

$\frac{\partial F}{\partial F_1}$ = the partial derivative of Equation 24 with respect to the force of load cell 1

ΔF_1 = the uncertainty in the measurement of load cell 1

$\frac{\partial F}{\partial F_2}$ = the partial derivative of Equation 24 with respect to the force of load cell 2

ΔF_2 = the uncertainty in the measurement of load cell 2

$\frac{\partial F}{\partial F_3}$ = the partial derivative of Equation 24 with respect to the force of load cell 3

ΔF_3 = the uncertainty in the measurement of load cell 3

$\frac{\partial F}{\partial F_4}$ = the partial derivative of Equation 24 with respect to the force of load cell 4

ΔF_4 = the uncertainty in the measurement of load cell 4

$\frac{\partial F}{\partial F_5}$ = the partial derivative of Equation 24 with respect to the force of load cell 5

ΔF_5 = the uncertainty in the measurement of load cell 5

$\frac{\partial F}{\partial F_6}$ = the partial derivative of Equation 24 with respect to the force of load cell 6

ΔF_6 = the uncertainty in the measurement of load cell 6

Equation 26 shows the equation to calculate the uncertainty in the magnitude of forces measurement.

Equation 26:

$$\Delta MF = \left[\left(\frac{F_1}{(F_1^2+F_2^2+F_3^2+F_4^2+F_5^2+F_6^2)^{\frac{1}{2}}}\Delta F_1\right)^2+\left(\frac{F_2}{(F_1^2+F_2^2+F_3^2+F_4^2+F_5^2+F_6^2)^{\frac{1}{2}}}\Delta F_2\right)^2+\left(\frac{F_3}{(F_1^2+F_2^2+F_3^2+F_4^2+F_5^2+F_6^2)^{\frac{1}{2}}}\Delta F_3\right)^2+\left(\frac{F_4}{(F_1^2+F_2^2+F_3^2+F_4^2+F_5^2+F_6^2)^{\frac{1}{2}}}\Delta F_4\right)^2+\left(\frac{F_5}{(F_1^2+F_2^2+F_3^2+F_4^2+F_5^2+F_6^2)^{\frac{1}{2}}}\Delta F_5\right)^2+\left(\frac{F_6}{(F_1^2+F_2^2+F_3^2+F_4^2+F_5^2+F_6^2)^{\frac{1}{2}}}\Delta F_6\right)^2\right]^{\frac{1}{2}}$$

Table 14: Fall 2010 load cell uncertainty

Run #	Magnitude Force Uncertianty (lb)	Horizontal Force Uncertianty (lb)	Vertical Force Uncertianty (lb)
1	0.150	0.230	0.171
2	0.150	0.306	0.532
3	0.150	0.218	0.128
4	0.150	0.139	0.143
5	0.150	0.352	0.346
6	0.150	0.189	0.215
7	0.150	0.467	0.525
8	0.150	0.444	0.391

Table 15: Summer 2011 load cell uncertainty

Run #	Magnitude Force Uncertianty (lb)	Horizontal Force Uncertianty (lb)	Vertical Force Uncertianty (lb)
1	0.15	0.226	0.273
2	0.15	0.321	0.389
3	0.15	0.254	0.339
4	0.15	0.269	0.273
5	0.15	0.202	0.224
6	0.15	1.448	0.291
7	0.15	0.225	0.224
8	0.15	0.494	0.745
9	0.15	0.233	0.561
10	0.15	0.461	0.458
11	0.15	1.204	0.699
12	0.15	0.249	0.249
13	0.15	0.273	0.294
14	0.15	0.255	0.246
15	0.15	1.061	1.041
16	0.15	0.223	0.306
17	0.15	0.513	0.777

Table 16: Fall 2011 load cell uncertainty

Run #	Magnitude Force Uncertainty (lb)	Horizontal Force Uncertainty (lb)	Vertical Force Uncertainty (lb)
1	0.159	0.429	0.382
2	0.153	0.406	0.292
3	0.160	0.620	0.472
4	0.153	0.607	0.368
5	0.153	0.555	0.322
6	0.156	0.447	0.259
7	0.150	0.476	0.327
8	0.149	0.567	0.466
9	0.136	0.412	0.288
10	0.150	0.540	0.417
11	0.147	0.486	0.448
12	0.148	0.354	0.294
13	0.155	0.603	0.417
14	0.148	0.403	0.269
15	0.154	0.650	0.425
16	0.156	0.491	0.422
17	0.142	0.336	0.265
18	0.148	0.330	0.237
19	0.157	0.484	0.440
20	0.082	0.398	0.426
21	0.141	0.450	0.404
22	0.144	0.579	0.510
23	0.137	0.312	0.315
24	0.145	0.474	0.298
25	0.133	0.228	0.242
26	0.143	0.482	0.349
27	0.145	0.324	0.331
28	0.133	0.518	0.400
29	0.139	0.343	0.393
30	0.140	0.569	0.433